Robust optimal ship hulls based on Michell's wave resistance

Salah-Eddine Zerrouq, Morgan Pierre

ROBUST OPTIMAL SHIP HULLS BASED ON MICHELL'S WAVE RESISTANCE

SALAH-EDDINE ZERROUQ AND MORGAN PIERRE

Abstract. We seek the hull of a ship with a given volume which minimizes the water resistance with uncertainties on the cruising speed. The water resistance is based on Michell's wave resistance functional and the speed is a random variable whose probability distribution is known. We first handle the case where the support of the hull is given, and then we also optimize this support for a given area. In each case, an optimal hull is shown to exist. The numerical simulations are costly so we adapt to our problem Newton's method for shape optimization. The numerical results are compared to the case where the cruising speed is known.

Keywords: Michell's wave resistance, Dirichlet energy, probability distribution, robust deterministic control, geometric shape optimization, Newton's method, lumped mass matrix.
Mathematics Subject Classification: 49J55, 49M15, 65K10, 76B20.

1. Introduction

In this paper, we are interested in optimizing the hydrodynamic properties of a ship. In this regard, the most famous feature for minimizing the water resistance to the motion of a ship is perhaps the bulbous bow, a protruding bulb at the front of the ship, just beneath the waterline [12]. Schematically speaking, the wave created by the bulb cancels the wave created by the bow of the ship; this reduces the wake and the energy lost in creating it. However, a bulbous bow is generally optimized for a cruising speed and it is generally not optimal for other speeds. Here, we want to find a hull which is optimal for a range of speeds.

The starting point in our approach is a simplified model in which the water resistance is the sum of a wave resistance (related to the wake of the ship) and of a viscous resistance (related to friction between the water and the hull of the ship). Such a decomposition is standard in ship hydrodynamics [5], but we focus here on a specific model where, for a given form of the hull and for a given speed, the wave resistance is computed by Michell's formula [25] and the viscous resistance is proportional to the wetted surface of the hull and to the square of the speed.

In Michell's formula, which is based on a linear potential flow theory, a function represents half of the wetted hull and the other half is obtained by symmetry. In [10], the problem of finding a half hull function which minimizes the total resistance for a given speed of the ship and a given volume of the hull was solved both theoretically and numerically. In this case, the domain of definition of the hull function was also given (for instance, a rectangle, as in the Wigley hulls [26]). This unified former

S. Zerrouq: Arts et Métiers ParisTech, I2M CNRS UMR 5295, F-33400 Talence, France
M. Pierre: Laboratoire de Mathématiques et Applications, Université de Poitiers, CNRS, F-86073 Poitiers, France

results from the literature. In particular, the existence and uniqueness result of Krein and Sizov [21, 31] was extended to a Sobolev setting and the famous bulbous bow was recovered numerically for moderate values of the speed, as in [20, 24].

In [8, 9], the more modern question of optimizing also the domain of definition of the hull function, for a given area, was considered. An optimal support was proved to exist, assuming for compactness that all the admissible supports belonged to a bounded hold-all domain. Several numerical simulations showed again the presence of a bulbous bow in a specific speed regime.

The simulations above pointed out that the shape of the bulb is very sensitive to the speed of the ship. Our purpose here is to propose a more robust model in which the variations or incertainties in the cruising speed are taken into account. Thus, we assume that the speed is a random variable whose probability distribution is known and we minimize the *expectation of the total resistance* for a given volume of the hull. We shall use a deterministic algorithm to compute the minimizer. In control theory, this approach is known as a robust deterministic control (see, e.g., [2, p.469, case (d)]). As previously, we will consider two situations. First, we handle the case where the domain of definition of the hull is fixed, and secondly we optimize this domain of definition, for a given area.

We first explain our model based on Michell's formula and on a given probability distribution of the speed in Section 2. Then, in Section 3, we consider the situation where the domain of definition of the hull function is fixed. We prove the existence and uniqueness of an optimal hull with given volume. We also establish the regularity of this optimal hull when the domain is a rectangle. Numerical simulations are given for two different kinds of probability distributions. Because of the averaging process, the bulbous bow is no longer present in the robust hull.

In Section 5, we optimize the support of the optimal hull for a given area. We prove the existence of an optimal support and then we focus on numerical simulations. In order to reduce the computational time, we adapt to our problem Newton's method for shape optimization. This is a technical matter because of the complex form of second order shape derivatives, so we first explain our discretization on several model problems in Section 4.

In the context of shape optimization, Newton's method is scarce in the literature because of its complexity. It was first implemented in [29], where the authors give a discretization of the second order shape derivative as a full matrix. We also refer to [17] where the author uses a conjugate gradient method to compute the inverse of the Hessian matrix at every iteration. More recently, a level-set approach was developed in [3, 37].

For our problem, we use a geometric shape optimization approach with a fitted mesh and a $\mathbb{P}_1$ finite element discretization. The use of a trapezoidal rule for the numerical integration on the boundary allows us to deal only with a *diagonal* Hessian matrix. This diagonal matrix reminds the method of lumped masses used for the finite element approximation of parabolic problems [34, Chapter 15]. It can also be regarded as a quasi-Newton method. This is detailed in Section 4 for the Dirichlet energy. A similar discretization is used for our optimal design problem in Section 5. The numerical results show that the robust hull obtained by this approach still has a bulbous bow, even if the averaging process has a smoothing effect on the geometry of the hull.

2. The formal optimal design problems

The total resistance of water to the motion of a ship is the force required to tow the ship in calm water a constant speed. A traditional and simplified approach (see, e.g., [5]) uses the decomposition

$$R_{total} = R_{wave} + R_{viscous}. \tag{2.1}$$

The wave resistance reflects the energy that goes into creating the wave.

In 1898, Michell [25] gave a formula for the wave resistance, valid for any shape of the hull, for a constant speed and in an infinite domain. Experiments starting with Wigley in the 1920's showed a reasonable good agreement between theory and experiment (see the review by Gotman [14] and references therein). We first recall Michell's formula and then we give a simple formula for the viscous resistance.

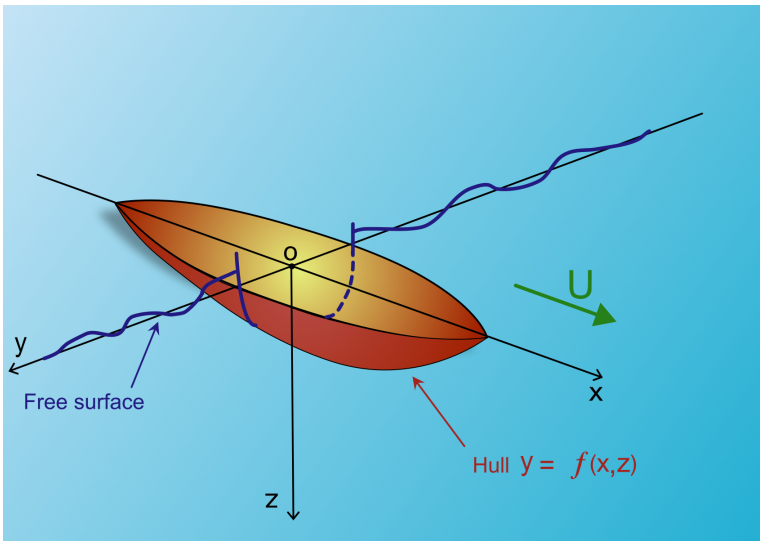

FIGURE 1. The immerged hull: half of it is represented by a positive function $y = f(x, z)$. The other half hull is obtained by symmetry.

2.1. **Michell's wave resistance formula.** Consider a ship moving with constant speed U on the surface of an unbounded fluid. We assume that the coordinates xyz are fixed to the ship: the xy-plane is the water surface and z is vertically **downward**. The immerged half hull surface is represented by a continuous nonnegative function (see Figure 1)

$$y = f(x, z) \geq 0, \quad (x, z) \in \overline{D}.$$

The set $\overline{D}$ on which f is defined is split into three parts: its interior D (an open subset of the upper half-plane with a Lipschitz boundary), in which $f(x, z) > 0$, its boundary Γ_N at the surface $z = 0$ and its boundary Γ_0 under the surface, on which $f(x, z) = 0$ (see Figure 2).

It is assumed that the fluid is incompressible, inviscid and that the flow is irrotational. The motion has lasted long enough so that a steady state has been reached.

Michell's formula [25] reads

$$R_{wave} = \frac{4\rho g^2}{\pi U^2} \int_1^\infty (I_1(\lambda)^2 + I_2(\lambda)^2) \frac{\lambda^2}{\sqrt{\lambda^2 - 1}} d\lambda, \tag{2.2}$$

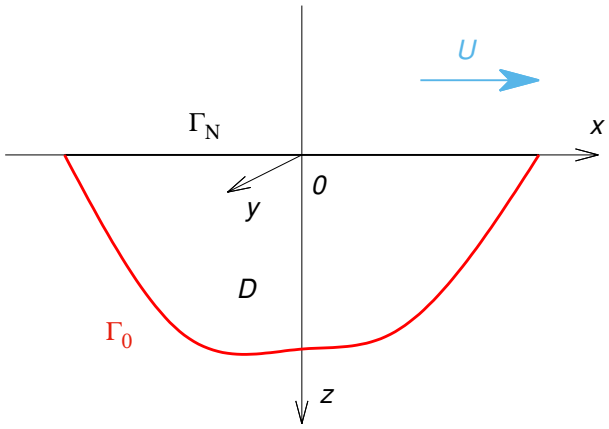

FIGURE 2. The domain of parameters (x, z)

with

$$I_1(\lambda) = \int_D \frac{\partial f(x,z)}{\partial x} \exp\left(-\frac{\lambda^2 g z}{U^2}\right) \cos\left(\frac{\lambda g x}{U^2}\right) dxdz, \tag{2.3}$$

$$I_2(\lambda) = \int_D \frac{\partial f(x,z)}{\partial x} \exp\left(-\frac{\lambda^2 g z}{U^2}\right) \sin\left(\frac{\lambda g x}{U^2}\right) dxdz. \tag{2.4}$$

In this formula, U (in $\mathrm{m}\cdot\mathrm{s}^{-1}$) is the speed of the ship, ρ (in $\mathrm{kg}\cdot\mathrm{m}^{-3}$) is the constant density of the fluid and g (in $\mathrm{m}\cdot\mathrm{s}^{-2}$) is the standard gravity. The variables x, z and $f(x, z)$ are expressed in meters. Consequently, the integrals $I_1(\lambda)$ and $I_2(\lambda)$ are in m^2 and R_{wave} (in Newton) has the dimension of a force.

The integration parameter λ has no dimension: it can be interpreted as $\lambda = 1/\cos\theta$, where θ is the angle between the ship's path and the direction of wave propagation [5, p. 310], [35]. For $\theta = 0$ ($\lambda = 1$), waves follow the ship with their crests aligned perpendicular to the ship's course (transverse waves) and for $\theta = \pm\pi/2$ ($\lambda = +\infty$), waves have crests parallel to the ship's path.

We stress that Michell's approach is a linear theory in which the ship is assumed to be "thin", which means that the angles made by the hull surface with the longitudinal plane of symmetry are small, i.e.

$$0 \le f \ll 1, \quad \left|\frac{\partial f}{\partial x}\right| \ll 1 \quad \text{and} \quad \left|\frac{\partial f}{\partial x}\right| \ll 1 \quad \text{in } D. \tag{2.5}$$

In our approach, we do not assume the conditions (2.5) *a priori*, but we will recover them in a weak form by penalizing these constraints thanks to the viscous resistance.

Remark 2.1. In Michell's model, the flow is irrotational and incompressible, so we seek a potential in the form $-Ux + \phi$ where ϕ is small and satisfies

$$\begin{cases} -\Delta\phi & = 0 \quad \text{in } \mathbb{R}\times\mathbb{R}_+\times\mathbb{R}_+ \text{ (a quarter space)}, \\ \partial_{xx}\phi - \dfrac{g}{U^2}\partial_z\phi & = 0 \quad \text{on } z = 0, \\ \partial_y\phi + U\partial_x f & = 0 \quad \text{on } y = 0^+. \end{cases} \tag{2.6}$$

In (2.6), the first equation is the incompressibility condition whereas the third equation is a linearization of the impermeability condition on the hull. The second equation is known as the Neumann-Kelvin condition [22]. It is obtained by combining a linearized no-slip condition and a linearized Bernoulli equation at the free surface.

In [25], Michell managed to compute a physical solution to problem (2.6) which satisfies the condition $\lim_{x\to+\infty} |\nabla\phi| = 0$. This means that in front of the ship, there is no wake. The wave resistance is the drag force in this model and it is computed as

$$-2\int_{\mathbb{R}^2} \delta p \partial_x f(x,z) dxdz,$$

where $\delta p = \rho U \partial_x \phi(x,0,z)$ stands for the difference of pressure due to the ship.

In [32], Sretensky solved problem (2.6) in the case of a finite depth H by means of a Fourier transform. He recovered Michell's wave resistance formula by letting H tend to infinity.

2.2. **The viscous resistance and the total resistance.** In formula (2.1), a traditionnal approach is to express the viscous resistance as (see, e.g., [5])

$$R_{viscous} = \frac{1}{2}\,\rho U^2\, C_F\, A\,. \tag{2.7}$$

The viscous resistance $R_{viscous}$ accounts for the effects of viscosity which are not present in Michell's model. In (2.7), C_F is the viscous drag (or friction) dimensionless coefficient and A (in m^2) is the surface area of the ship's wetted hull. The coefficient C_F can sometimes have a complicated form [5] but throughout this manuscript, we assume that C_F is a positive constant.

Since the graph of f represents the ship's half-hull, A is given by:

$$A = 2\int_D \sqrt{1+|\nabla f(x,z)|^2}\, dxdz. \tag{2.8}$$

For a thin ship, $|\nabla f|$ is uniformly small (see (2.5)), and the integral above can be approximated by performing a Taylor expansion of $\sqrt{1+|\nabla f|^2}$ at first order:

$$A = 2\int_D 1 dxdz + \int_D |\nabla f(x,z)|^2\, dxdz + o(||\nabla f||_\infty^2)\,. \tag{2.9}$$

A good approximation of the viscous drag for small ∇f reads

$$R_{viscous} = \frac{1}{2}\rho U^2\, C_F \left(2|D| + \int_D |\nabla f(x,z)|^2\, dxdz\right), \tag{2.10}$$

where $|D|$ is the area of D.

Summing up, the total resistance for a ship hull defined by f reads

$$R_{total} = R_{wave} + R_{viscous}, \tag{2.11}$$

where R_{wave} is defined by (2.2)-(2.4) and $R_{viscous}$ is defined by (2.10). In this formula, the cruising speed of the ship, U, is constant.

2.3. **The formal optimal design problems.** The variables g and ρ are known physical constants and we assume for simplicity that the viscous drag coefficient C_F is a given constant. Then the total resistance defined by (2.11), (2.2) and (2.10) depends only on the function $f : \overline{D} \to \mathbb{R}$ and on the speed U, so we write $R_{total}(f,U)$. The half volume of the hull (a positive real number) is given and it is denoted by $\mathcal{V}$.

2.3.1. *Robust optimization of the hull for a given domain.* In [10], Dambrine, Pierre and Rousseaux solved the following convex problem for a fixed domain D, by using an appropriate H^1 functional setting: for a given speed $U > 0$,

$$\begin{cases} \text{Find the function } f_D \text{ which minimizes } R_{total}(f,U) \text{ in the set} \\ \left\{ f : \overline{D} \to \mathbb{R},\ f = 0 \text{ on } \Gamma_0 \text{ and } \int_D f(x,z)dxdz = \mathcal{V} \right\}. \end{cases} \tag{2.12}$$

The solution to this problem may be very sensitive to variations of U. In order to have a more robust problem, we assume now that U is a random function with realizations denoted by U_ω and we consider the problem:

$$\begin{cases} \text{Find the function } f_D^\star \text{ which minimizes } \mathbb{E}(R_{total}(f,U)) \text{ in the set} \\ \left\{ f : \overline{D} \to \mathbb{R},\ f = 0 \text{ on } \Gamma_0 \text{ and } \int_D f(x,z)dxdz = \mathcal{V} \right\}. \end{cases} \tag{2.13}$$

It will be interesting to compare $R_{total}(f_D^\star, U)$ with $R_{total}(f_D, U)$.

The cost function $R_{total}(f,U)$ can more generally be replaced by

$$J(f,U) = h(U) \times R_{total}(f,U)$$

where $h : (0,+\infty) \to (0,+\infty)$ is a continuous function of U. For instance, we may choose

- $h(U) = UT$ where T is a time, in which case $J(f,U)$ is an energy;
- $h(U) = 1$, in which case $J(f,U)$ is the total resistance.

Remark 2.2. Since Michell's wave resistance is computed for a steady state, this model means that in the term $\mathbb{E}(h(U)R_{total}(f,U))$, we neglect the transitory states between two steady states.

Remark 2.3. It would be more natural to add the condition $f \geq 0$ in the set of functions for problem (2.12), in order to avoid self-crossing of the hull, as in [10]. Here, we will check this condition numerically. That is, we first solve problem (2.12), a quadratic-linear minimization problem which reduces to a linear problem (cf. (3.16)), and we check *a posteriori* that $f_D \geq 0$ in D. The same approach holds for problem (2.13).

2.3.2. *Robust optimization of the domain and of the hull.* Next, we consider the domain D as a variable of the problem. The total resistance is written $R_{total}(D, f_D, U)$ where for a given domain D and a given speed $U > 0$, f_D is the solution to problem (2.12). We fix an area $a > 0$. In [8, 9], Dambrine and Pierre studied the following shape optimization problem: for a given constant speed U,

$$\begin{cases} \text{Find a set } D_U \text{ which minimizes } R_{total}(D, f_D, U) \\ \text{among all bounded regular open subsets } D \text{ of the lower half-plane} \\ \text{such that } |D| = a. \end{cases} \tag{2.14}$$

Here and below, $|D|$ is the area of the domain D. Let h be a positive continuous function of U. Since U is fixed, $h(U)$ is a constant and we may use the cost function $h(U)R_{total}(D, f_D, U)$ in the problem above without changing its solution(s) D_U.

Now we assume again that U is a random function and we are interested in the more robust problem:

$$\begin{cases} \text{Find a set } D^\star \text{ which minimizes } \mathbb{E}\left[h(U)R_{total}(D, f_D, U)\right] \\ \text{among all bounded regular open subsets } D \text{ of the lower half-plane} \\ \text{such that } |D| = a. \end{cases} \tag{2.15}$$

For the numerical resolution of problem 2.15 in Section 5.2, we will compute the first order and second order shape derivatives of the set functional. For its theoretical resolution in Section 5.1, we will seek for an optimal support rather than an optimal domain.

3. Robust optimal hull for a fixed domain

3.1. **Functional setting.** Let D be a bounded and connected open subset of the upper half plane $\{(x, z) \in \mathbb{R}^2 \ : \ z > 0\}$. We assume that D has a Lipschitz boundary ∂D. For the sake of simplicity, we also assume throughout section 3 that the part of ∂D which intersects the x-axis, namely $\partial D \cap (\mathbb{R} \times \{0\})$, is a segment of the x-axis (possibly empty). We let Γ_N denote the relative interior of this segment and $\Gamma_0 = \partial D \setminus \Gamma_N$.

We work with the Sobolev space

$$H(D) = \left\{u \in H^1(D) \ : \ u = 0 \text{ on } \Gamma_0 \text{ in the sense of traces}\right\}.$$

Let $u \in H(D)$ (u is the hull function) and $V > 0$ (V is the speed of the ship). For Michell's wave resistance, we set

$$\alpha = \frac{g}{V^2} \tag{3.1}$$

and (2.2) becomes

$$R_{wave}(u, \alpha) = \frac{4\rho g\alpha}{\pi} \int_1^\infty |S_u(\lambda)|^2 \frac{\lambda^2}{\sqrt{\lambda^2 - 1}} d\lambda,$$

with (cf. (2.3)-(2.4))

$$S_u(\lambda, u, \alpha) = \int_D \frac{\partial u}{\partial x}(x, z) e^{-i\lambda\alpha x} e^{-\lambda^2 \alpha z} dxdz.$$

The number α is known as the *Kelvin wave number*. The value $1/\alpha$ (in m) is the typical wavelength of the transverse waves. Transverse waves follow the ship with their crests and troughs aligned perpendicular to the ship's course and the wavelength is the distance between two successive crests. Since the speed V of the ship can be recovered from α through $V = \sqrt{g/\alpha}$, knowing α is equivalent to knowing V. We will use the variable α because it is more convenient.

Integrating S_u by parts with respect to x and taking advantage of the boundary condition $u = 0$ on $\partial\Omega$, we find that

$$R_{wave}(u, \alpha) = \frac{4\rho g\alpha^3}{\pi} \int_1^\infty |T(u, \alpha, \lambda)|^2 \frac{\lambda^4}{\sqrt{\lambda^2 - 1}} d\lambda, \tag{3.2}$$

where, for all $\lambda > 0$,

$$T(u, \alpha, \lambda) = \int_D u(x, z) e^{-i\lambda\alpha x} e^{-\lambda^2 \alpha z} dxdz.$$

The viscous resistance (2.10) reads

$$R_{viscous}(u,\alpha) = \frac{\rho g}{2\alpha} C_F \left(2|D| + \int_D |\nabla u(x,z)|^2 \, dxdz \right).$$

The total resistance is

$$R_{total}(u,\alpha) = R_{viscous}(u,\alpha) + R_{wave}(u,\alpha). \tag{3.3}$$

We assume that the Kelvin wave number is a random variable $\nu : \Omega \to \mathbb{R}$ on a complete probability space $(\Omega, \mathcal{A}, \mathbb{P})$. Moreover, we assume that the probability distribution $\mathbb{P}_\nu$ of ν is a measure which has a compact support in $(0, +\infty)$. We recall that the probability distribution of ν is defined for every Lebesgue-measurable set $B \subset \mathbb{R}$ by

$$\mathbb{P}_\nu(B) = \mathbb{P}(\nu \in B) = \mathbb{P}\left(\{w \in \Omega \ : \ \nu(\omega) \in B\}\right).$$

Concerning the Kelvin wave number, ν denotes the random variable, whereas α is a positive real number.

We recall that if $X : \Omega \to \mathbb{R}$ is a random variable which is integrable with respect to $\mathbb{P}$, its expectation is defined by

$$\mathbb{E}(X) = \int_\Omega X(\omega) d\mathbb{P}(\omega).$$

If $\varphi : (0, +\infty) \to \mathbb{R}$ is a continuous function, then $\varphi(\nu) : \Omega \to \mathbb{R}$ is a random variable and we have the well-known formula,

$$\mathbb{E}[\varphi(\nu)] = \int_\Omega \varphi(\nu(\omega)) d\mathbb{P}(\omega) = \int_{\mathbb{R}} \varphi(s) d\mathbb{P}_\nu(s).$$

In view of (3.3), we consider the cost function

$$\mathcal{J}_D(u) = \mathbb{E}\left[h_{\rho,g,C_F}(\nu) \big(R_{viscous}(u,\nu) + R_{wave}(u,\nu) \big) \right], \tag{3.4}$$

where $h_{\rho,g,C_F} : (0, +\infty) \to (0, +\infty)$ is a continuous function which may depend on the physical constants ρ, g and on the viscous coefficient C_F. We note that it could be interesting to consider C_F as a random variable as well (possibly dependent on α), but we assume for simplicity that C_F is constant.

Following [9], we introduce the normalized viscous resistance functional

$$J_0(u) = \int_D |\nabla u|^2 dxdz$$

and the normalized wave resistance functional

$$J_{wave}(u,\alpha) = \frac{8\alpha^4}{\pi} \int_1^\infty |T(u,\alpha,\lambda)|^2 \frac{\lambda^4}{\sqrt{\lambda^2 - 1}} d\lambda, \tag{3.5}$$

where T is defined as previously for all $u \in H(D)$, $\alpha > 0$ and $\lambda > 0$ by

$$T(u,\alpha,\lambda) = \int_D u(x,z) e^{-i\lambda\alpha x} e^{-\lambda^2 \alpha z} dxdz. \tag{3.6}$$

The cost function (3.4) reads

$$\mathcal{J}_D(u) = \mathbb{E}\left[h_{\rho,g,C_F}(\nu) \frac{\rho g}{2\nu} C_F \left(2|D| + J_0(u) + \frac{1}{C_F} J_{wave}(u,\nu) \right) \right].$$

By setting

$$\tilde{h}(\alpha) = h_{\rho,g,C_F}(\alpha) \frac{\rho g}{2\alpha} C_F, \tag{3.7}$$

we have

$$\mathcal{J}_D(u) = \mathbb{E}\left[\tilde{h}(\nu)\left(2|D| + J_0(u) + \frac{1}{C_F}J_{wave}(u,\nu)\right)\right]. \tag{3.8}$$

We note that $\tilde{h}$ generally depends on the fixed parameters ρ, g and C_F.

We let $\mathcal{V} > 0$ denote the half-volume of the hull. We consider the set

$$H_{\mathcal{V}}(D) = \left\{u \in H(D) \ : \ \int_D u\,dxdz = \mathcal{V}\right\},$$

which is a closed affine subspace of $H(D)$. Our robust optimization problem reads:

$$\text{Find } u_D^\star \in H_{\mathcal{V}}(D) \text{ such that } \mathcal{J}_D(u_D^\star) = \min\left\{\mathcal{J}_D(u) \ : \ u \in H_{\mathcal{V}}(D)\right\}. \tag{3.9}$$

In (3.9), the set D is given and the positive parameters ρ, g, C_F and $\mathcal{V}$ are fixed.

3.2. **Theoretical results.** The following result will prove useful.

Lemma 3.1. *Let $q \in (1,+\infty)$ and let $q' = q/(q-1) \in (1,+\infty)$ denote the conjugate exponent of q. Assume that $H \in L^q(D\times D)$. Then for all $u, v \in L^{q'}(D)$, we have*

$$\int_{D\times D} |H(x,z,x',z')u(x,z)v(x',z')|dxdzdx'dz' \le \|H\|_{L^q(D\times D)}\|u\|_{L^{q'}(D)}\|v\|_{L^{q'}(D)}. \tag{3.10}$$

Moreover, for each $u \in L^{q'}(D)$, the function

$$(x,z) \mapsto \int_D H(x,z,x',z')u(x',z')dx'dz' \tag{3.11}$$

belongs to $L^q(D)$.

Proof. Estimate (3.10) is a consequence of Hölder's inequality. The claim on the function (3.11) follows from (3.10), Fubini's theorem and a duality argument. □

By formally switching the integrals in the expression (3.5)-(3.6), we see that Michell's normalized wave resistance can be written

$$J_{wave}(u,\alpha) = \int_{D\times D} k_\alpha(x,z,x',z')u(x,z)u(x',z')dxdzdx'dz' \tag{3.12}$$

where

$$k_\alpha(x,z,x',z') = \frac{8\alpha^4}{\pi}K(\alpha(x-x'),\alpha(z+z')) \tag{3.13}$$

and

$$K(X,Z) = \int_1^\infty e^{-\lambda^2 Z}\cos(\lambda X)\frac{\lambda^4}{\sqrt{\lambda^2-1}}d\lambda. \tag{3.14}$$

This formal calculation was rigorously proved in [8, Appendix A]. It was shown that Michell's kernel belongs to $L^{5/4-\varepsilon}(D\times D)$ and that this estimate is optimal if D contains a half-disk centered on the x-axis.

The results from [8, Appendix A] are summarized in the proposition below. We first note that K is defined and continuous on $\mathbb{R}\times(0,+\infty)$, thanks to the exponential term, so that k_α is continuous on $(\mathbb{R}\times(0,+\infty))^2$.

Proposition 3.2. *Let $\alpha > 0$. Michell's normalized wave resistance kernel k_α (3.13) belongs to $L^q(D\times D)$ for all $1 \le q < 5/4$. For each $q' > 5$ and for each $u \in L^{q'}(D)$, the formulations for $J_{wave}(u)$ given by (3.5)-(3.6) and (3.12)-(3.13)-(3.14) are equal.*

Let $q \in (1, 5/4)$ and let $q' = q/(q-1) \in (5, +\infty)$ be the conjugate exponent of q. Since $H^1(D)$ is continuously imbedded in $L^{q'}(D)$ for all $q' \in [1 + \infty)$ [1], Proposition 3.2 and Lemma 3.1 show that for all $u \in H(D)$, $J_{wave}(u) < +\infty$.

The following result is proved in [9, Lemma 5.2 (ii)].

Lemma 3.3. *For each $u \in H(D)$, the map*

$$\alpha \mapsto J_{wave}(u, \alpha)$$

is continuous on $(0, +\infty)$.

Recall that $\mathbb{P}_\nu$ has a compact support in $(0, +\infty)$, so we may assume that its support is included in $[\nu_{min}, \nu_{max}]$ with $0 < \nu_{min} \leq \nu_{max} < +\infty$. We define the kernel

$$H_\nu(x, z, x', z') = \int_{\nu_{min}}^{\nu_{max}} \tilde{h}(s) k_s(x, z, x', z') d\mathbb{P}_\nu(s),$$

which has finite values for all $(x, z, x', z') \in D \times D$ (since $z + z' > 0$).

Proposition 3.4. *The kernel H_ν belongs to $L^q(D \times D)$ for all $1 \leq q < 5/4$ and for all $u \in H(D)$, we have*

$$\mathbb{E}\left[\tilde{h}(\nu) J_{wave}(u, \nu)\right] = \int_{D \times D} H_\nu(x, z, x', z') u(x, z) u(x', z') dx dz dx' dz'. \tag{3.15}$$

Proof. We choose $q \in (1, 5/4)$ and we denote by $q' \in (5, +\infty)$ the conjugate exponent of q. Since the function $t \mapsto t^{q'}$ is convex on $[0, +\infty)$, by Jensen's inequality, we have

$$\left|H_\nu(x, z, x', z')\right|^{q'} \leq \int_{\nu_{min}}^{\nu_{max}} \tilde{h}^{q'}(s) |k_s(x, z, x', z')|^{q'} d\mathbb{P}_\nu(s).$$

Thus, by (3.13) and Fubini's theorem,

$$\begin{aligned}
&\int_{D \times D} \left|H_\nu(x, z, x', z')\right|^{q'} dx dz dx' dz' \\
&\qquad \leq \int_{\nu_{min}}^{\nu_{max}} \int_{D \times D} \hat{h}(s) |K(s(x - x'), s(z + z'))|^{q'} dx dz dx' dz' d\mathbb{P}_\nu(s),
\end{aligned}$$

where $\hat{h} : (0, +\infty) \to (0, +\infty)$ is a continuous function, namely

$$\hat{h}(s) = \tilde{h}^{q'}(s) \left(\frac{8 s^4}{\pi}\right)^{q'}.$$

We perform the change of variable $(\tilde{x}, \tilde{z}, \tilde{x}', \tilde{z}') = (sx, sz, sx', sz')$ and we find

$$\begin{aligned}
&\int_{D \times D} \left|H_\nu(x, z, x', z')\right|^{q'} dx dz dx' dz' \\
&\qquad \leq \int_{D \times D} |K(x - x', z + z')|^{q'} dx dz dx' dz' \int_{\nu_{min}}^{\nu_{max}} \frac{1}{s^4} \hat{h}(s) d\mathbb{P}_\nu(s),
\end{aligned}$$

In the right handside above, the first integral is finite thanks to Proposition 3.2. The second integral is finite since $[\nu_{min}, \nu_{max}]$ is compactly embedded in $(0, +\infty)$. This proves that H_ν belongs to $L^{q'}(D \times D)$. For the computation of

$$\mathbb{E}\left[\tilde{h}(\nu) J_{wave}(u, \nu)\right],$$

we use the expression (3.12). The estimates above combined with Hölder's inequality (as in (3.10)) show that we may apply apply Fubini's theorem. This yields (3.15). □

Remark 3.1. Let $\alpha_0 > 0$ and assume that $\mathbb{P}_\nu$ is the Dirac delta function at α_0, δ_{α_0}. Then the kernel H_ν is simply

$$H_\nu(x,z,x',z') = \tilde{h}(\alpha_0) k_{\alpha_0}(x,z,x',z').$$

We are in position to prove:

Theorem 3.5. *Problem* (3.9) *has a unique solution* $u_D^\star$ *which is also the unique solution in* $H^1(D)$ *of the boundary value problem*

$$\begin{cases} -\Delta u(x,z) + \dfrac{1}{C_F \mathbb{E}\left[\tilde{h}(\nu)\right]} \displaystyle\int_{D\times D} H_\nu(x,z,x',z') u(x',z') dx'dz' = C, \ \forall (x,z) \in D, \\ \int_D u \, dxdz = \mathcal{V}, \\ u = 0 \ \text{on} \ \Gamma_0, \\ \dfrac{\partial u}{\partial n} = 0 \ \text{on} \ \Gamma_N. \end{cases} \tag{3.16}$$

Proof. The functional T defined by (3.6) depends linearly on its first argument u, so that for each $\alpha > 0$, $u \mapsto J_{wave}(u,\alpha)$ is a quadratic and convex functional on $H(D)$. Thus, $u \mapsto \mathbb{E}(\tilde{h}(\nu) J_{wave}(u,\nu))$ defined by (3.5) is convex on $H(D)$. On the other hand, the function J_0 is stricly convex on $H(D)$, thanks to the homogeneous Dirichlet boundary condition on Γ_0 and the Poincaré inequality. Thus, $\mathcal{J}_D$ is stricly convex on $H(D)$ and since $H_\mathcal{V}(D)$ is an affine subspace of $H(D)$, problem (3.9) has a most one solution in $H_\mathcal{V}(D)$.

Let (u_n) be a minimizing sequence for problem (3.9) in $H_\mathcal{V}(D)$. We have

$$\mathcal{J}_D(u_n) = \mathbb{E}\left[\tilde{h}(\nu) 2|D|\right] + \mathbb{E}\left[\tilde{h}(\nu)\right] J_0(u_n) + \frac{1}{C_F}\mathbb{E}\left[\tilde{h}(\nu) J_{wave}(u_n,\nu)\right].$$

Each one of the three terms in the right hand-side is nonnegative so $\mathcal{J}_D(u_n)$ is nonnegative and the sequence (u_n) is bounded in $H^1(D)$ (thanks to the term $J_0(u_n)$ and the Poincaré inequality). Up to a subsequence, (u_n) converges weakly in $H^1(D)$ to some $u_D^\star$, which belongs to $H_\mathcal{V}(D)$ since the latter is a closed convex subset of $H^1(D)$. By lower semi-continuity of J_0,

$$J_0(u_D^\star) \leq \liminf_n J_0(u_n).$$

Now, let $q' \in (5, +\infty)$. The space $H^1(D)$ is compactly embedded in $L^{q'}(D)$ [1] so (u_n) converges strongly to $u_D^\star$ in $L^{q'}(D)$. By Proposition 3.4,

$$\mathbb{E}\left[\tilde{h}(\nu) J_{wave}(u_n,\nu)\right] \to \mathbb{E}\left[\tilde{h}(\nu) J_{wave}(u_D^\star,\nu)\right].$$

Thus, $\mathcal{J}_D(u_D^\star) \leq \liminf_n \mathcal{J}_D(u_n)$. since (u_n) is a minimizing sequence, this proves that $u_D^\star$ is a minimizer.

The Euler-Lagrange equation associated to problem (3.9) yields the boundary value problem (3.16). The constant C in the first line is the Lagrange multiplier associated to the volume constraint $\int_D u dxdz = \mathcal{V}$. Conversely, each solution to (3.16) is a critical point of $\mathcal{J}_D$ on $H_\mathcal{V}(D)$ and by convexity, it is a minimizer. This concludes the proof. □

Remark 3.2. In particular, the statement of Theorem 3.5 is true if $\mathbb{P}_\nu = \delta_{\alpha_0}$ for some $\alpha_0 > 0$. This means that the ship has a constant speed. In this case, $H_\nu = \tilde{h}(\alpha_0)k_{\alpha_0}$ (see Remark 3.1). The same holds for Proposition 3.6 and Theorem 3.7 below.

Proposition 3.6. *If D is symmetric with respect to z-axis, then $u_D^\star$ is even with respect to x.*

Proof. Since D is symmetric with respect to the z-axis, for all $(x,z) \in D$, we have $(-x,z) \in D$. Let $\check{u} \in H(D)$ be defined by

$$\check{u}(x,z) = u_D^\star(-x,z), \quad \forall (x,z) \in D.$$

Performing the change of variable $x \mapsto -x$ in $T(\check{u},\alpha,\lambda)$ (see (3.6)), we find that

$$T(\check{u},\alpha,\lambda) = \int_D u_D^\star(x,z) e^{i\lambda\alpha x} e^{-\lambda^2 \alpha z} dxdz.$$

Thus,

$$|T(\check{u},\alpha,\lambda)| = |T(u_D^\star,\alpha,\lambda)|$$

and consequently, by (3.5),

$$J_{wave}(\check{u},\alpha) = J_{wave}(u_D^\star,\alpha), \quad \forall \alpha > 0.$$

Similarly, we have $J_0(\check{u}) = J_0(u_D^\star)$ and so

$$\mathcal{J}_D(\check{u}) = \mathcal{J}_D(u_D^\star).$$

Since $\check{u}$ belongs to $H_\nu(D)$, this shows that $\check{u}$ is a solution to problem (3.9). By uniqueness of the solution, $\check{u} = u_D^\star$. □

Theorem 3.7. *If D is a rectangle, then the solution $u_D^\star$ to problem* (3.9) *belongs to $W^{2,5/4-\varepsilon}(D)$ for all $\varepsilon > 0$ small enough.*

Proof. Let $q \in (1, 5/4)$. Since $u_D^\star$ belongs to $H^1(D)$ which is continously embedded in $L^{q'}(D)$, we deduce from (3.16), Proposition 3.4 and Lemma 3.1 that $u_D^\star$ solves the PDE

$$-\Delta u_D^\star + f = C \text{ in } D,$$

where f belongs to $L^q(D)$ and C is constant. The domain D is a rectangle and $u_D^\star$ satisfies homogeneous Dirichlet boundary conditions on three sides and homogeneous Neumann boundary conditions on one side. By elliptic regularity on polygons [15], $u_D^\star$ belongs to $W^{2,q}(D)$. □

3.3. **Numerical simulations.** In this section, we present numerical results for the optimal hulls which minimize the expectation of the total resistance (3.3).

3.3.1. *The two optimal design problems.* The cost function is

$$\begin{aligned} \mathcal{J}_D(u) &= \mathbb{E}\left(R_{total}(u,\nu)\right) \\ &= \mathbb{E}\left(R_{viscous}(u,\nu) + R_{wave}(u,\nu)\right). \end{aligned}$$

In other words, we choose $h_{\rho,g,C_F}(\alpha) = 1$ or equivalently (cf. (3.7))

$$\tilde{h}(\alpha) = \frac{\rho g}{2\alpha} C_F \tag{3.17}$$

in the cost function $\mathcal{J}_D$ defined by (3.8). The domain D is a rectangle whose upper side is on the x-axis. We recall that the robust optimization problem (3.9) reads

$$\text{Find } u_D^\star \in H_\nu(D) \text{ such that } \mathcal{J}_D(u_D^\star) = \min\left\{\mathcal{J}_D(u) \ : \ u \in H_\nu(D)\right\}. \tag{3.18}$$

We shall compare the optimal hull $u_D^\star$ with the solution to the following (non robust) optimization problem:

$$\text{Find } \bar{u}_D \in H_{\mathcal{V}}(D) \text{ such that } R_{total}(\bar{u}_D, \alpha) = \min\left\{R_{total}(u,\alpha) \ : \ u \in H_{\mathcal{V}}(D)\right\}, \tag{3.19}$$

where the value α is set to $\alpha = \mathbb{E}(\nu)$. By Remark 3.2, problem (3.19) has a unique solution. We shall also compare these optimal hulls with standard Wigley hulls (see, e.g., [26]).

Problem (3.19) was investigated numerically in [10] (see also references therein). We have also computed the optimal hull $\bar{u}_D$ for different values of α. The domain is a rectangle with length $L = 2.2\,\mathrm{m}$ and draft $T = 0.3\,\mathrm{m}$. The half volume of the hull is $\mathcal{V} = 0.06\,\mathrm{m}^3$. The other parameters are

$$\rho = 1000\,\mathrm{kg}\cdot\mathrm{m}^{-3}, \quad g = 9.81\,\mathrm{m}\cdot\mathrm{s}^{-1} \quad \text{and} \quad C_F = 0.01. \tag{3.20}$$

For the space discretization of the problem, we used a P_1 finite element approach (see Section 3.3.2). A triangulation of the rectangular domain into 1956 triangles and 1075 vertices was used.

It is convenient to introduce the length Froude number

$$Fr_L = \frac{V}{\sqrt{gL}} = \frac{1}{\sqrt{\alpha L}}, \tag{3.21}$$

which is a dimensionless version of the speed V.

With these parameters, we have recovered the results from [10]. Namely, for intermediate Froude numbers $Fr_L \in [0.5, 1]$, the hull has the famous *bulbous bow*, which reduces the contribution of the wave resistance in the total resistance. A bulbous bow is seen in Figure 5 (bottom) for $Fr_L = 0.6$.

For large or small Froude numbers ($Fr_L > 1$ or $Fr_L < 0.5$), the influence of Michell's wave resistance is small and the optimal hull $\bar{u}_D$ mainly minimizes the viscous resistance. Figure 3 (bottom) shows $\bar{u}_D$ for $Fr_L = 0.277$.

3.3.2. *Numerical approximation.* The expectation of the water resistance $\mathcal{J}_D(u)$ is given by

$$\begin{aligned}\mathcal{J}_D(u) &= \mathbb{E}\left[\tilde{h}(\nu)\Big(2|D| + J_0(u) + \frac{1}{C_F}J_{wave}(u,\nu)\Big)\right] \\ &= 2\mathbb{E}[\tilde{h}(\nu)]|D| + \mathbb{E}[\tilde{h}(\nu)]J_0(u) + \frac{1}{C_F}\mathbb{E}[\tilde{h}(\nu)J_{wave}(u,\nu)].\end{aligned}$$

By dropping the constant term, we see that minimizing $\mathcal{J}(u)$ is the same as minimizing

$$\tilde{\mathcal{J}}_D(u) = \int_D |\nabla u|^2 dxdz + \frac{1}{C_F\mathbb{E}[\tilde{h}(\nu)]}\int_{D\times D} H_\nu(x,z,x',z')u(x,z)u(x',z')dxdzdx'dz'. \tag{3.22}$$

By Theorem 3.5, a minimizer $u_D^\star$ of $\tilde{\mathcal{J}}_D(u)$ in $H_{\mathcal{V}}(D)$ is a solution to the linear boundary value problem (3.16).

To solve this problem, we adopt a finite element approach, in the sense that the optimal hull $u_D^\star$ is sought in a finite dimensional space

$$\mathcal{V}_h \subset H(D) \subset H^1(D).$$

Given a basis of P_1 (continuous and piecewise linear) finite elements $\{\phi_1, \phi_2, \ldots, \phi_n\}$, we can write

$$\text{for all } u_h \in \mathcal{V}_h, \quad u_h = \sum_{i=1}^{n} u_i \phi_i. \tag{3.23}$$

Then we have the following discretization of $\tilde{\mathcal{J}}_D(u_h)$:

$$\tilde{\mathcal{J}}_D(u_h) = U^t \Big(M_0 + \frac{1}{C_F \mathbb{E}[\tilde{h}(\nu)]} M_w \Big) U, \tag{3.24}$$

where $U = (u_1, \ldots, u_n)^t$ is the vector of the coordinates of u_h and M_0, M_w are matrices approximating J_0 and $u_h \mapsto \mathbb{E}[\tilde{h}(\nu) J_{wave}(u_h, \nu)]$. This yields the following discrete optimization problem:

$$u_D^\star = \operatorname{argmin} \left\{ U^t \Big(M_0 + \frac{1}{C_F \mathbb{E}[\tilde{h}(\nu)]} M_w \Big) U \ : \ u_h \in \mathcal{V}_h, \ \int_D u_h dx dz = \mathcal{V} \right\}. \tag{3.25}$$

The computation of the stiffness matrix

$$M_0 = \left(\int_D \nabla \phi_i \cdot \nabla \phi_j dx dz \right)_{1 \le i,j \le n}$$

is standard. This matrix M_0 is symmetric and positive definite. It is also sparse and non-diagonal.

The matrix M_w is symmetric and positive semi-definite, but in contrast to M_0, M_w is a full matrix because it is related to a nonlocal operator. Let us explain briefly how M_w is computed. Before discretizing, we write

$$\begin{aligned} \mathbb{E}[\tilde{h}(\nu) J_{wave}(u, \nu)] &= \mathbb{E}[R_{wave}(u, \nu)] \\ &= \frac{4\rho g}{\pi} \mathbb{E}\left[\nu^3 \int_1^\infty |T(u, \nu, \lambda)|^2 \frac{\lambda^4}{\sqrt{\lambda^2 - 1}} d\lambda \right] \\ &= \frac{4\rho g}{\pi} \int_{\nu_{\min}}^{\nu_{\max}} \alpha^3 f(\alpha) \int_1^\infty |T(u, \alpha, \lambda)|^2 \frac{\lambda^4}{\sqrt{\lambda^2 - 1}} d\lambda d\alpha \end{aligned}$$

where $T(u, \alpha, \lambda)$ is given by (3.6) and f is the probability density function of ν on the interval $[\nu_{min}, \nu_{max}] \subset (0, +\infty)$.

The approximation of the integral is done as follows. For a given (α, λ), the integral

$$T(u_h, \alpha, \lambda) = \int_D u_h(x, z) \exp(-i\lambda\alpha x - \lambda^2 \alpha z) dx dz$$

is computed by exact integration over each triangle of the mesh which approximates the domain D. The integration over α is handled by a numerical integration (the trapezoidal rule).

Concerning the density f, we consider two situations:

- A continuous uniform probability distribution for the Kelvin number on $[\nu_{min}, \nu_{max}]$, in which case

$$f(\alpha) = \frac{1}{\nu_{max} - \nu_{min}} \text{ on } [\nu_{min}, \nu_{max}]; \tag{3.26}$$

- A continuous uniform probability distribution for the speed $V = \sqrt{g/\alpha}$, as in (3.30).

For a given $\alpha > 0$ and $u_h \in \mathcal{V}_h$, the approximation of the integral

$$\int_1^\infty |T(u_h, \alpha, \lambda)|^2 \frac{\lambda^4}{\sqrt{\lambda^2 - 1}} d\lambda$$

is the same as in [10]. In particular, we use the value

$$\int_1^2 \frac{1}{\sqrt{\lambda^2 - 1}} = \ln(2 + \sqrt{3})$$

as in [33] to remove the singularity at $\lambda = 1$. The integral is also truncated at $+\infty$ and we use an appropriate midpoint formula for the remainder of the integral.

3.3.3. *Numerical results.* The parameters L, T, $\mathcal{V}$, ρ, g and C_F are the same as in Section 3.3.1. The probability distribution of the Kelvin wave number $\nu = g/V^2$ has a compact support included in $[\nu_{\min}, \nu_{\max}]$ with $0 < \nu_{\min} < \nu_{\max} < +\infty$. The bounds $\nu_{\min}, \nu_{max}$ are chosen so that the corresponding length Froude numbers are $Fr_{L_{\min}} = 0.2$ and $Fr_{L_{\max}} = 1$. Thus, we have

$$\nu_{\min} = \frac{1}{Fr_{L_{\max}}^2 L} = 0.45 \quad \text{and} \quad \nu_{\max} = \frac{1}{Fr_{L_{\min}}^2 L} = 11.36.$$

The case of a continuous uniform distribution of the Kelvin wave number. In this case, the density f is given by (3.26). The mean value of ν is

$$\mathbb{E}[\nu] = (\nu_{max} + \nu_{min})/2 = 5.90. \tag{3.27}$$

This corresponds to a Froude number equal to $Fr_L = 0.277$. Since Fr_L is a decreasing function of α (see (3.21)), the distribution of Froude numbers is concentrated near 0.2.

Figure 3 gives the shapes of the computed optimal hulls $u_D^\star$ (middle) and $\bar{u}_D$ (bottom). The top figure represents a Wigley hull w with triangular cross section and parabolic horizontal section, which is defined by [26, 33]

$$f(x, z) = \frac{B}{2}\left(1 - \frac{z}{T}\right)\left(1 - \frac{4x^2}{L^2}\right), \quad (x, z) \in [-L/2, L/2] \times [0, T]. \tag{3.28}$$

The beam B of w is chosen such that

$$\int_D w(x, z) dx dz = \frac{BLT}{6} = \mathcal{V}. \tag{3.29}$$

Namely, $B = 6\mathcal{V}/(LT) = 0.5454\,\text{m}$.

The three hulls have a very similar shape. We also note that the optimal hulls are symmetric back and front, in agreement with Proposition 3.6. However, they perform quite differently. This can be seen in Figure 4 which represents, for each hull, the total resistance (in Newton) on the range of Froude numbers $[0.2, 1.0]$. We stress that the constant term $2\tilde{h}(\alpha)|D|$ is not represented in this figure (see (3.22)). For each hull, the expectation of the total resistance is also given.

As expected, $u_D^\star$ clearly has the best expectation on the total range $[0.2, 1.0]$ (24 N for $u_D^\star$, 33 N for the Wigley hull w and 36 N for $\bar{u}_D$).

In contrast, $\bar{u}_D$ has the minimal total resistance for the mean Froude number $Fr_L = 0.277$. The hull $\bar{u}_D$ is even optimal among the three shapes for $Fr_L \in [0.2, 0.31]$. This is mainly due to a small contribution of the wave resistance in this interval. Interestingly, the expectation of the Wigley hull w is slightly better than the expectation of $\bar{u}_D$: a bulbous bow is interesting only in a limited range of speeds.

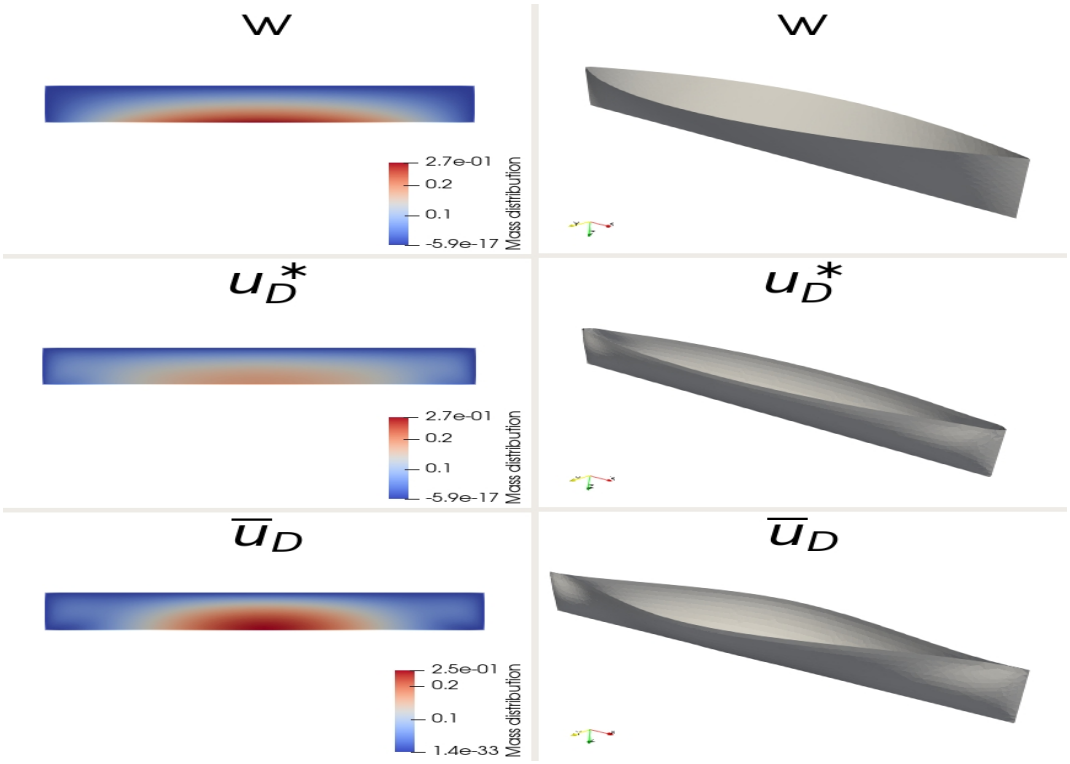

FIGURE 3. Mass distribution (left), and 3D results (right) of the Wigley hull w (top), the optimal hull $u_D^\star$ (middle, optimized for a uniform distribution of ν) and the optimal hull $\bar{u}_D$ (bottom, optimized for $\alpha = \mathbb{E}[\nu]$ with ν uniform).

The case of a continuous uniform distribution of the speed. We consider now a uniform distribution of the speed V on the interval $[V_{\min}, V_{\max}]$, corresponding to the Froude interval $[0.2, 1]$. Namely, we take

$$V_{\min} = 0.2\sqrt{gL} = 0.93 \quad \text{and} \quad V_{\max} = \sqrt{gL} = 4.64.$$

The mean value of the Froude number is obviously $Fr_L = 0.6$.

By an appropriate change of variables, we see that $\nu = g/V^2$ has a probability density given by

$$f(\alpha) = \frac{\sqrt{g/\alpha}}{2\alpha(V_{\max} - V_{\min})} \quad \text{on} \quad [\nu_{min}, \nu_{max}]. \tag{3.30}$$

Figure 5 shows the computed optimal hulls $u_D^\star$, $\bar{u}_D$ and the Wigley hull w. There is a striking difference between $\bar{u}_D$, which has a bulbous bow, and $u_D^\star$, which has no bulbous bow and looks like a Wigley hull.

The hydrodynamic properties of each hull appear clearly in Figure 6 which represents, for each hull, the total resistance on the range of Froude numbers $[0.2, 1.0]$ (up to the constant term $2\tilde{h}(\alpha)|D|$). The expectation of the total resistance is best for $u_D^\star$ (83 N), as expected. It is much better than for the Wigley hull w (128 N), but it is surprisingly very close to the expectation of $\bar{u}_D$ (84 N).

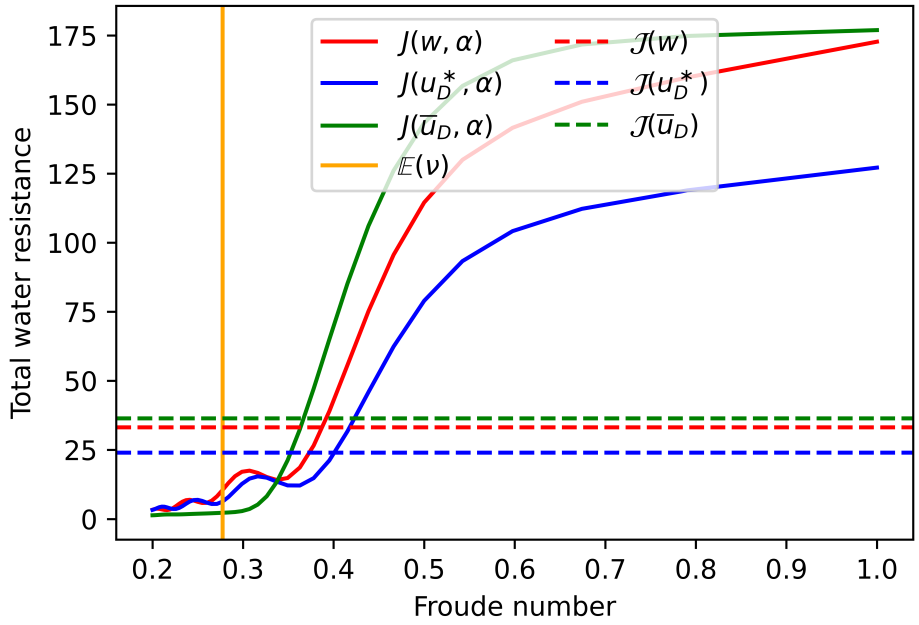

FIGURE 4. Total water resistance (in N) for the three hulls $u_D^\star$, $\bar{u}_D$ and w (case of a uniform distribution of ν).

For each hull, the total resistance is the sum of the viscous resistance and of the wave resistance. Since the viscous resistance is proportional to V^2 (cf. (2.10)), it is interesting to introduce for a given hull u the ratio

$$C_{viscous}(u) = \frac{1}{Fr_L^2}\left(R_{viscous}(u,\alpha) - 2\tilde{h}(\alpha)|D|\right),$$

which does not depend on α.

We have

$$C_{viscous}(u_D^\star) = 25\,\mathrm{N}, \quad C_{viscous}(w) = 33\,\mathrm{N} \quad \text{and} \quad C_{viscous}(\bar{u}_D) = 62\,\mathrm{N}.$$

Thus, $\bar{u}_D$ has the worst viscous resistance for every speed: a bulbous bow is clearly not optimal at high speed (Fr_L close to 1). At the mean speed $Fr_L = 0.6$, $\bar{u}_D$ has a better total resistance than $u_D^\star$ and w because it has a much better wave resistance. For $Fr_L \in [0.2, 0.4]$, $u_D^\star$ has a better total resistance than $\bar{u}_D$ and this is due to the wave resistance since the difference in the viscous resistance between the two hulls is less than $(62-25)\times 0,4^2 \approx 6\,\mathrm{N}$. For each hull, we notice the well-known oscillations of Michell's wave resistance for $Fr_L < 0.4$.

4. Newton's method for shape optimization

In this section, we first explain Newton's method for shape optimization in the continuous version. Then, we describe its discretization along with numerical exemples in the case of a PDE-fee example, before adapting it to the case of the Dirichlet energy. This is known as an *optimize-then-discretize* approach.

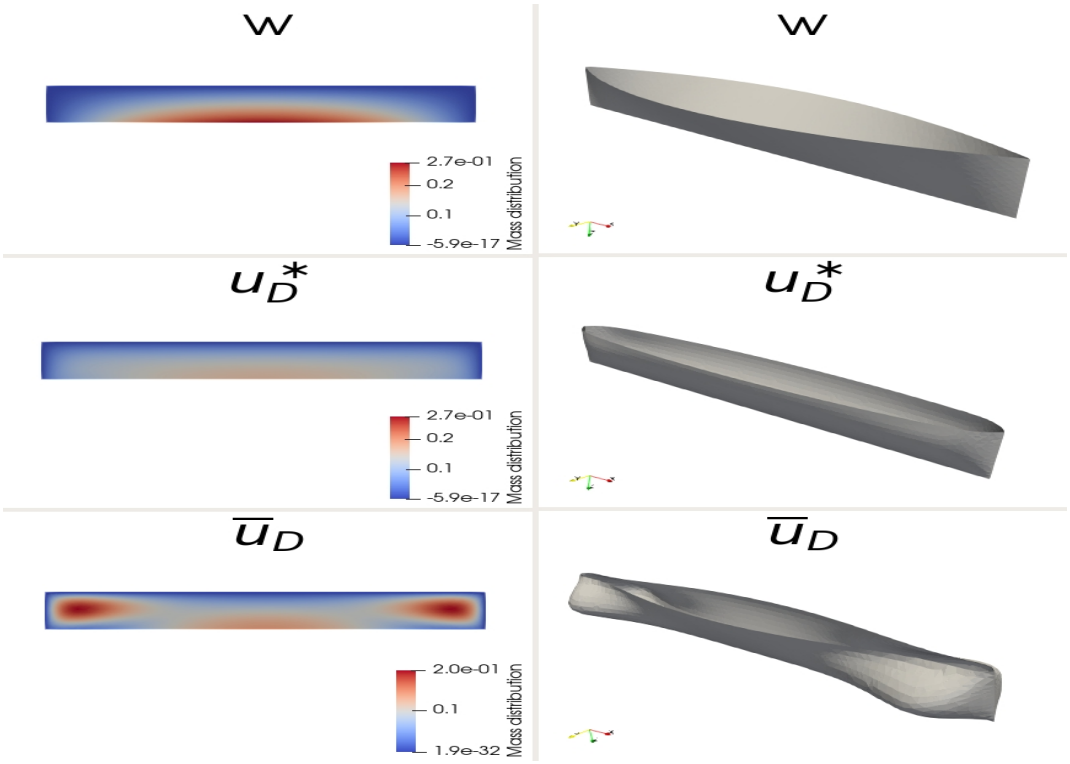

FIGURE 5. Mass distribution (left), and 3D results (right) of the Wigley hull w (top), the optimal hull $u_D^\star$ (middle, optimized for a uniform distribution of V) and the optimal hull $\bar{u}_D$ (bottom, optimized for $\alpha = \mathbb{E}[\nu]$ with V uniform).

4.1. **The continuous version.** For $k \geq 1$, $W^{k,\infty}(\mathbb{R}^2;\mathbb{R}^2)$ denotes the usual Sobolev space based on $L^\infty(\mathbb{R}^2;\mathbb{R}^2)$. In particular, $W^{1,\infty}(\mathbb{R}^2;\mathbb{R}^2)$ is the space of bounded Lipschitz continuous functions from $\mathbb{R}^2$ into $\mathbb{R}^2$. In order to work with classical derivatives, we consider for $k \geq 1$ the space

$$C^{k,\infty}(\mathbb{R}^2;\mathbb{R}^2) = C^k(\mathbb{R}^2;\mathbb{R}^2) \cap W^{k,\infty}(\mathbb{R}^2;\mathbb{R}^2),$$

endowed with the norm of $W^{k,\infty}(\mathbb{R}^2;\mathbb{R}^2)$.

For $k \in \mathbb{N}$, $\mathcal{O}_k$ is the set of bounded open subsets of $\mathbb{R}^2$ that are of class C^k. The first order shape derivative is defined classically as follows [37, Definition 3.2.11].

Definition 4.1. Let $k \geq 1$ and $E(\Omega)$ be a function from $\mathcal{O}_k$ into $\mathbb{R}$. We define

$$\begin{array}{rccl} \mathcal{E} \,:\, C^{k,\infty}(\mathbb{R}^2;\mathbb{R}^2) & \to & \mathbb{R} \\ \theta & \mapsto & E\left((Id+\theta)(\Omega)\right). \end{array}$$

The function E is said to be shape-differentiable at Ω if $\mathcal{E}$ is Fréchet-differentiable at 0, that is, if there exists a continuous linear map $\mathcal{E}'(0;\cdot) : C^{k,\infty}(\mathbb{R}^2;\mathbb{R}^2) \to \mathbb{R}$ such that

$$\mathcal{E}(\theta) = \mathcal{E}(0) + \mathcal{E}'(0;\theta) + o\left(\|\theta\|_{C^{k,\infty}(\mathbb{R}^2;\mathbb{R}^2)}\right).$$

We denote $E'(\Omega;\theta) = \mathcal{E}'(0;\theta)$.

The second order shape derivative is defined as follows [37, Definition 3.2.12].

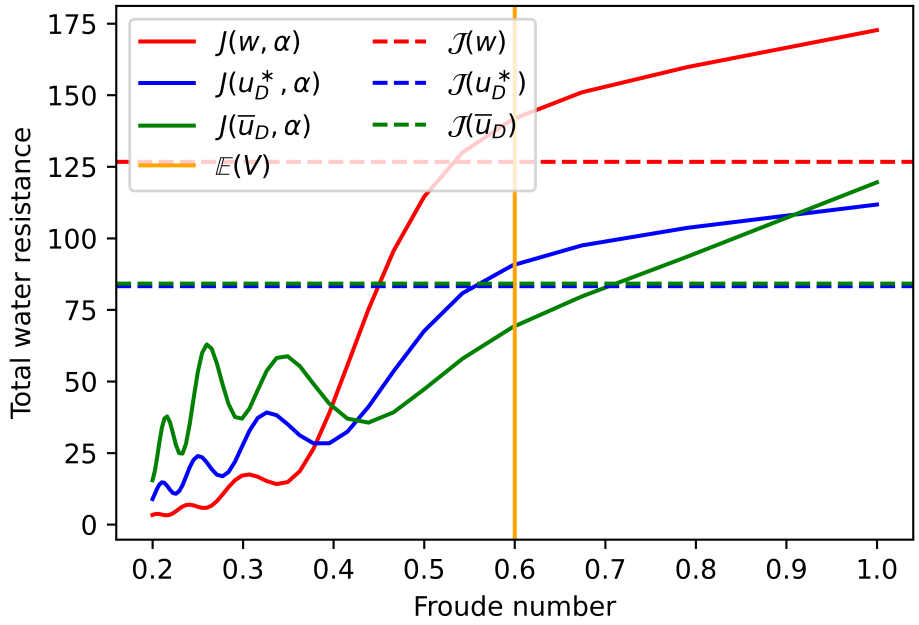

FIGURE 6. Total water resistance (in N) for the hulls $u_D^\star$, $\bar{u}_D$ and w (case of a uniform distribution of the speed V).

Definition 4.2. The function E of Definition 4.1 is said to be twice shape-differentiable at Ω if $\mathcal{E}'$ is Fréchet-differentiable in a neighborhood $\mathcal{U}$ of 0 in $C^{k,\infty}(\mathbb{R}^2;\mathbb{R}^2)$ and if the first derivative $\mathcal{E}'$ defined by

$$\begin{array}{rcl} \mathcal{E}' \ : \ \mathcal{U} & \to & \left(C^{k,\infty}(\mathbb{R}^2;\mathbb{R}^2)\right)' \\ \theta & \mapsto & \mathcal{E}'(\theta;\cdot), \end{array}$$

is Fréchet-differentiable at 0. We denote by $\mathcal{E}''(0;\theta,\xi)$ the second Fréchet derivative at 0, θ and ξ being respectively the first and second directions of derivation. We also denote $E''(\Omega;\theta,\xi) := \mathcal{E}''(0;\theta,\xi)$.

A set $\Omega \in \mathcal{O}_k$ is a *critical shape* if $E'(\Omega;\theta) = 0$ for all $\theta \in C^{k,\infty}(\mathbb{R}^2;\mathbb{R}^2)$. In particular, a minimizer of E in $\mathcal{O}_k$ is a critical shape.

Formally, Newton's method for finding a critical shape reads as follows. Start from a set $\Omega_0 \in \mathcal{O}_k$ and for $p = 0, 1, 2, \ldots$ until convergence:

- Find $\theta_p \in C^{k,\infty}(\mathbb{R}^2;\mathbb{R}^2)$ such that

$$E^{''}(\Omega_p;\theta_p,\xi) = -E'(\Omega_p;\xi), \quad \forall \xi \in C^{k,\infty}(\mathbb{R}^2;\mathbb{R}^2); \tag{4.1}$$

- Set

$$\Omega_{p+1} = (Id + \theta_p)(\Omega_p) \tag{4.2}$$

If $\Omega \in \mathcal{O}_{k+1}$ and if $E : \mathcal{O}_k \to \mathbb{R}$ is shape differentiable at Ω, it is well-known since Hadamard [16] that $E'(\Omega;\theta)$ depends only on the trace of the normal component of θ on the boundary $\Gamma = \partial\Omega$ (see, e.g., [19, Proposition 5.9.1]). Moreover, if $\Omega \in \mathcal{O}_{k+2}$, then $E^{''}(\Omega;\cdot,\cdot)$ is not invertible because each vector field $\theta \in C^{k,\infty}(\mathbb{R}^2;\mathbb{R}^2)$ which has

compact support in $\mathbb{R}^2 \setminus \Gamma$ belongs to the kernel of $E''(\Omega;\cdot,\cdot)$. This is a consequence of the structure theorem of $E''(\Omega;\cdot,\cdot)$ [28].

Thus, we solve equation (4.1) for vector fields θ, ξ defined on Γ. Since a small perturbation of Γ is fully defined by a normal deformation, in Newton's equation (4.1) we will seek $\theta_p \in C^{k,\infty}$ such that its tangential component on Γ, denoted by θ_Γ, is zero. Thus, (4.1) becomes

$$\begin{cases} \text{find } \theta \in C^{k,\infty}(\mathbb{R}^2;\mathbb{R}^2) \text{ such that } \theta_\Gamma = 0 \text{ and} \\ E''(\Omega;\theta,\xi) = -E'(\Omega;\xi), \quad \forall \xi \in C^{k,\infty}(\mathbb{R}^2;\mathbb{R}^2) \text{ such that } \xi_\Gamma = 0, \end{cases} \tag{4.3}$$

where we have omitted the subscript p for simplicity.

This approach simplifies $E''(\Omega;\theta,\xi)$ because it cancels the tangential components of θ and ξ which are otherwise present if Ω is sufficiently regular [28]. Moreover, this is a consistent approach. Indeed, the purpose is to converge to a critical shape $\Omega^\star$ and for a critical shape, $E''(\Omega^\star;\theta,\xi)$ depends only on the normal components of the traces of θ, ξ on Γ [19, Remark p. 246]. A related idea was used with Newton's algorithm for shape optimization in [3] in the context of a level-set discretization.

Thus, in order to solve problem (4.3), we first seek the normal component $\theta \cdot n$ on Γ. Then, we extend θ on Ω with a Hilbertian extension-regularization technique as described in [4, Section 5.2]. In our case, we used the inner product inherited from linear elasticity.

4.2. **PDE-free example.** Let $f \in C^3(\mathbb{R}^2;\mathbb{R})$. We consider the minimization problem

$$\inf_{\Omega \in \mathcal{O}_3} E(\Omega) \tag{4.4}$$

where

$$E(\Omega) = \int_\Omega f(x)dx$$

is the function to be minimized. With appropriate assumptions on f (see, e.g., [37, Proposition 3.3.5]), an optimal shape $\Omega^\star$ is explicitly given by the set of negative values of f,

$$\Omega^\star = \{x \in \mathbb{R}^2 \mid f(x) < 0\}. \tag{4.5}$$

We seek to compute $\Omega^\star$ by Newton's method, and we shall follow an optimize-then-discretize approach.

Assume that $\Omega \in \mathcal{O}_3$. Since f is smooth, the function $\mathcal{E}$ from Definition 4.1 is of class C^2 on $C^{1,\infty}(\mathbb{R}^2;\mathbb{R}^2)$ and the shape derivatives of $E(\Omega)$ are given by [19]

$$\begin{aligned} E'(\Omega;\xi) &= \int_\Gamma (\xi \cdot n) f, \\ E''(\Omega;\theta,\xi) &= \int_\Gamma (\theta \cdot n)(\xi \cdot n)\big(\mathcal{H} f + \partial_n f\big) + \int_\Gamma Z_{\theta,\xi} f, \end{aligned} \tag{4.6}$$

where Γ is the boundary of Ω, $\mathcal{H}$ is the mean curvature of Γ, and

$$Z_{\theta,\xi} = \theta_\Gamma \cdot D_\Gamma n\, \xi_\Gamma - \theta_\Gamma \cdot \nabla_\Gamma(\xi \cdot n) - \xi_\Gamma \cdot \nabla_\Gamma(\theta \cdot n). \tag{4.7}$$

For $\theta, \xi \in C^{1,\infty}(\mathbb{R}^2;\mathbb{R}^2)$ such that $\theta_\Gamma = 0$ and $\xi_\Gamma = 0$, we have $Z_{\theta,\xi} = 0$. Thus, Newton's equation (4.3) reads: find $\theta_n \in C^1(\Gamma)$ such that

$$\int_\Gamma \theta_n \xi_n \big(\mathcal{H} f + \partial_n f\big) = -\int_\Gamma \xi_n f, \quad \forall \xi_n \in C^1(\Gamma). \tag{4.8}$$

This problem has to be properly discretized. We explain our approach which allows to obtain a diagonal hessian matrix when working with $\mathbb{P}_1$ normal Lagrange finite element deformation vectors.

4.2.1. *Discretization of Newton's equation.* Given a conforming triangulation $\mathcal{T}_h$ of a polygonal domain Ω_h which approximates the domain Ω, Γ_h denotes the boundary of the mesh which consists of an ordered n_{be}-tuple of ordered vertices $(\mathbf{x}_1, \mathbf{x}_2, \dots, \mathbf{x}_{n_{be}})$. Let

$$\mathcal{V}_h = \left\{ u_h \in C(\Omega_h, \mathbb{R}) \;\middle|\; \forall T_i \in \mathcal{T}_h,\ u_{h|T_i} \in \mathbb{P}_1 \right\}$$

be the Lagrange finite element space of continuous functions that are piecewise polynomials of degree 1. We denote by $(\phi_i)_{1\le i\le N_h}$ the nodal basis of $\mathcal{V}_h$ defined by

$$\forall\, 1 \le i, j \le N_h,\ \phi_i(a_j) = \delta_{ij},$$

where N_h is the dimension of $\mathcal{V}_h$ and $(a_j)_{1\le j\le N_h}$ are the vertices of the triangulation $\mathcal{T}_h$. We denote by $n_h(\mathbf{x}_i)$ the discrete normal vector to the boundary at the vertex $\mathbf{x}_i$ which is approximated as the rotate of the tangent at $\mathbf{x}_i$, $\tau_h(\mathbf{x}_i) = \frac{\overrightarrow{\mathbf{x}_{i-1}\mathbf{x}_{i+1}}}{\left\|\overrightarrow{\mathbf{x}_{i-1}\mathbf{x}_{i+1}}\right\|}$ as shown in Figure 7.

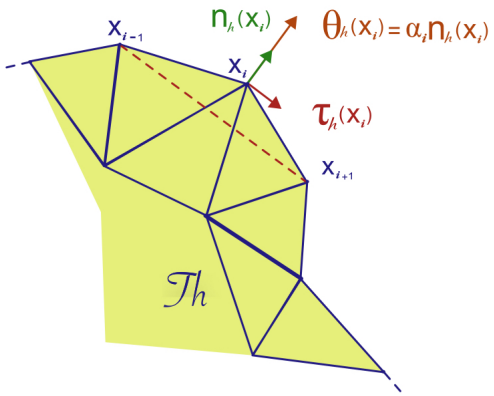

FIGURE 7. Discrete setting around a vertex $\mathbf{x}_i$

We search for a descent direction $\theta_h : \mathbb{R}^2 \to \mathbb{R}^2$ defined on the vertices of $\mathcal{T}_h$. Since (4.8) contains boundary integrals, we first compute the descent direction θ_h on the boundary vertices $\mathbf{x}_1, \dots, \mathbf{x}_{n_{be}}$ before extending it to all of the triangulation $\mathcal{T}_h$ through Hilbertian extension techniques (see [4]). We assume that θ_h is normal to the boundary Γ_h at every vertex $\mathbf{x}_i$, that is

$$\forall i = 1, \dots, n_{be},\ \exists \alpha_i \in \mathbb{R}, \quad \theta_h(\mathbf{x}_i) = \alpha_i n_h(\mathbf{x}_i). \tag{4.9}$$

We use the continuous piecewise linear ($\mathbb{P}_1$) extension of θ_h on Γ_h, namely

$$\theta_h(x) = \sum_{i=1}^{n_{be}} \alpha_i \varphi_i(x) n_h(\mathbf{x}_i), \tag{4.10}$$

where $(\varphi_i)_{1\le i\le n_{be}}$ is the nodal basis of continuous and piecewise linear functions on Γ_h defined by

$$\forall 1 \le i, j \le n_{be}, \quad \varphi_i(\mathbf{x}_j) = \delta_{ij}. \tag{4.11}$$

Here and below, κ denotes the discrete curvature computed by a standard formula (see, e.g., [38, Appendix A.3]). By choosing the normal deformation $\xi_h(x) = \varphi_i(x)n_h(\mathbf{x}_i)$, the discrete version of Newton's equation (4.8) is:

Find θ_h in the form (4.10) such that

$$\int_{\Gamma_h} \theta_h(x)\cdot n_h(\mathbf{x}_i)\varphi_i(x)\big(\kappa(x)f(x)+\partial_{n_h}f(x)\big) = -\int_{\Gamma_h} f(x)\varphi_i(x)n_h(\mathbf{x}_i)\cdot n_h(x), \quad (4.12)$$

for $i = 1, \dots, n_{be}$. Here $n_h(x) = \sum_{i=1}^{n_{be}} \varphi_i(x)n_h(\mathbf{x}_i)$ can be chosen as the $\mathbb{P}_1$ interpolate of the normal.

Another issue is the discretization of the boundary integral on Γ_h. This can be a major source of error and lack of consistency as noted in [37]. We choose a trapezoidal rule, which is known to converge rapidly for periodic smooth functions. In view of (4.11), equation (4.12) becomes

$$\alpha_i\big(\kappa(\mathbf{x}_i)f(\mathbf{x}_i) + \partial_{n_h}f(\mathbf{x}_i)\big) = -f(\mathbf{x}_i), \qquad \text{for } i = 1, \dots, n_{be}, \quad (4.13)$$

where we used that $\theta_h(\mathbf{x}_i)\cdot n_h(\mathbf{x}_i) = \alpha_i$ and where

$$\partial_{n_h}f(\mathbf{x}_i) = \nabla f(\mathbf{x}_i)\cdot n_h(\mathbf{x}_i). \quad (4.14)$$

Remark 4.1. Expression (4.14) requires the knowledge of ∇f. If we only know f, then we replace (4.14) with $\nabla^h f(\mathbf{x}_i)\cdot n_h(\mathbf{x}_i)$, where $\nabla^h f \in \mathcal{V}_h \times \mathcal{V}_h$ is the continuous $\mathbb{P}_1$-valued derivative of f defined by local least square problems as explained in Appendix A. We use this formula in the numerical examples which follow.

One can see that the system of equations (4.13) can be easily solved, since the left-hand side has a diagonal matrix which is invertible as long as it contains no zero entries. This reminds the method of lumped masses used for the finite element approximation of parabolic problems [34, Chapter 15]. In our case, we also deal with the normal deformations.

In conclusion, finding a discrete descent direction θ_h through Newton's equation boils down to solving the system of equations (4.13) for the values of α_i at each vertex, and taking

$$\forall i = 1, \dots, n_{be} \quad \theta(\mathbf{x}_i) = \alpha_i n_h(\mathbf{x}_i). \quad (4.15)$$

We stress that at each step (4.2) of Newton's algorithm, a filtering of the boundary mesh is necessary in order to compute correctly the discrete curvature. We used Savitsky-Golay filters (see [38, Appendix A.3]).

4.2.2. *Numerical examples.* Next, we compute the optimal shapes for problem (4.4) and for three different functions f_i, namely

$$f_1(x,y) = (x^2+y^2)^5 - 2a^5(x^5 - 10x^3y^2 + 5xy^4) + a^{10} - b^{10},$$

with $a = 0.95$, $b = 0.953$,

$$f_2(x,y) = ((x-0.5)^2+y^2)((x+0.5)^2+y^2) - 0.51^4,$$
$$f_3(x,y) = \max(x^2 - 0.6^2, y^2 - 0.6^2).$$

These functions were inspired by [37, Section 12.1].

The initial shape is a unit disc that we successively deform using the discretization (4.13) and a constant time step $t = 1$ (cf. (4.2)). The results are given in Figures 8-10.

One can see that the optimal shapes are easily computed after 7 iterations for f_1 and f_2. The convergence rate is very fast although it seems geometric rather than

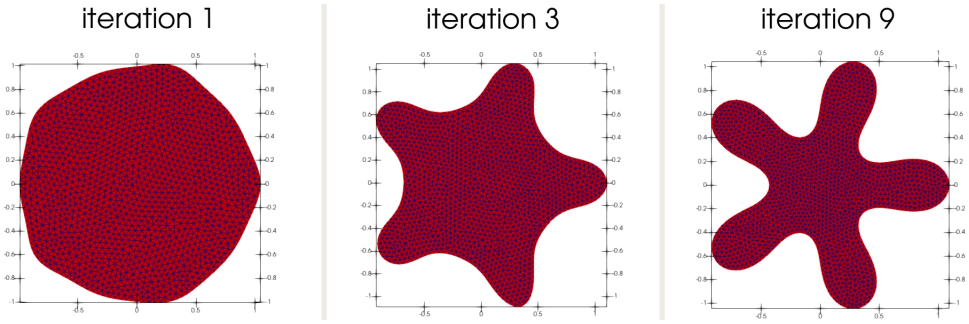

FIGURE 8. Optimal (right) and intermediate shapes (left and middle) for minimizing $E(\Omega, f_1)$

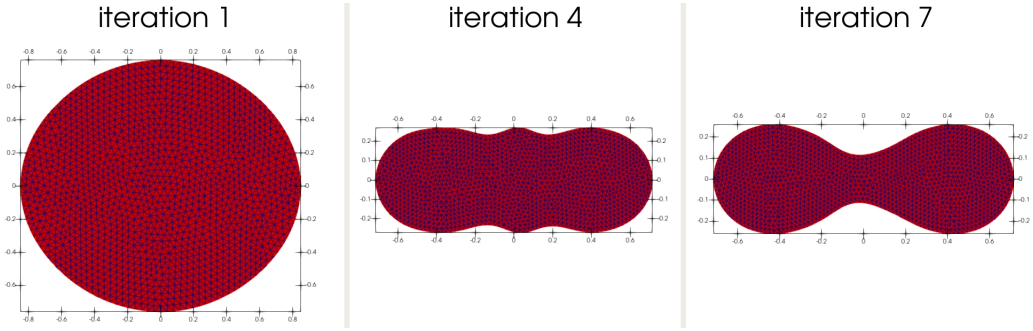

FIGURE 9. Optimal (right) and intermediate shapes (left and middle) for minimizing $E(\Omega, f_2)$

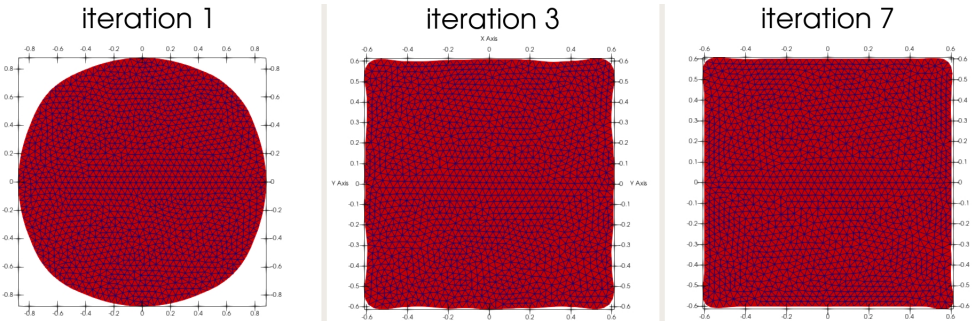

FIGURE 10. Optimal (right) and intermediate shapes (left and middle) for minimizing $E(\Omega, f_3)$

quadratic, as illustrated in Figure 11. Quadratic convergence rate has been observed in some specific examples [38, Section 8.1.2]

Figure 10 helps to illustrate an important issue with the computation of optimal shapes. The discretization (4.13) assumes that the optimal shapes are smooth, not only to be able to define the different discrete quantities necessary for the algorithm such as the normals to the boundary n_h, but also the structure of the second order shape derivative adopted in (4.6) is only valid for domains Ω that are at least C^3. Thus Newton's algorithm will fail to capture optimal shapes that contain corners or

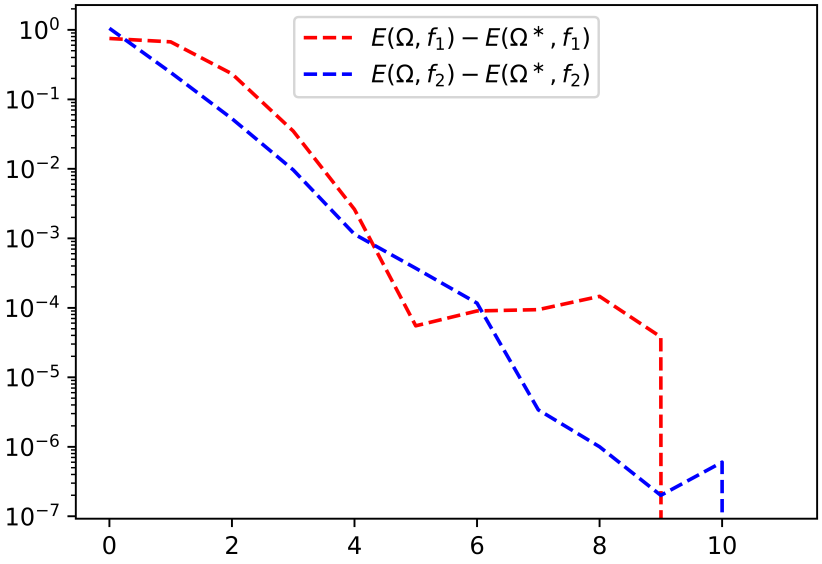

FIGURE 11. The error to the best shape $\Omega^\star$ at every iteration of the minimization process for the different functionals $E(\Omega, f_i)$

cusps. This is noticed in Figure 10 where the set of negative values f_3 is clearly a square, but the algorithm never captures the square and gets stuck oscillating around shapes close to a square.

This oscillation can be seen in Figure 12 where we give the $L^\infty(\Omega_h)$ norm of the computed descent directions θ_h. We see that $\|\theta_h\|_\infty$ converges rapidly for $E(\Omega, f_1)$ and $E(\Omega, f_2)$ after only 7 iterations. In contrast, for $E(\Omega, f_3)$, where the optimal shape is a square, we can see that while the value of the norms is low, it fails to converge and keeps on oscillating.

Moreover, Figure 12 shows that the L^∞ norm is constant around the optimal shape. Our experiments suggest that this can be taken as a stopping criterion for Newton's algorithm. This contrasts with first order algorithms where $\|\theta_h\|_\infty$ tends to oscillate around critical shapes.

4.3. **The Dirichlet energy.** We now consider a functional that depends on the domain Ω through the solution u of a PDE. We consider the case of the Dirichlet energy

$$E(\Omega) = \int_\Omega |\nabla u|^2, \tag{4.16}$$

where u is solution to the Dirichlet equation

$$\begin{cases} -\Delta u &= 1 \qquad \text{in } \Omega, \\ u &= 0 \qquad \text{on } \Gamma. \end{cases} \tag{4.17}$$

It is well known (see for example [7, 30, 36]) that the following shape optimization problem,

$$\max_{\substack{\Omega \in \mathcal{O}_3 \\ |\Omega| = m}} E(\Omega), \tag{4.18}$$

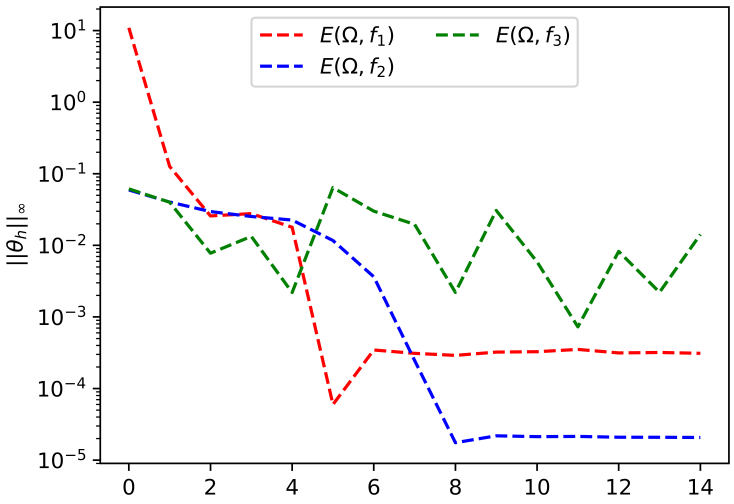

FIGURE 12. The $L^\infty(\Omega_h)$ norm of the computed descent direction θ_h at every iteration of the minimization process for the different functionals $E(\Omega, f_i)$

has a unique solution $\Omega^\star$ which is the disc of area m. Here $|\Omega| = \int_\Omega dx$ denotes the area of Ω.

We seek to compute this optimal shape $\Omega^\star$ with our algorithm and to this end, we need boundary expressions for the first and second order derivatives E' and E''. These derivatives have been extensively studied in shape optimization literature (see for example [19, 23] and references therein). Here, we give the expressions in a way suited to our discretization (see [38, Section 8.2.1] or [19, Section 5.9.6]). We have:

Theorem 4.1. *Let $\Omega \in \mathcal{O}_3$. Then the Dirichlet energy $E(\Omega)$ defined in (4.16) is twice shape differentiable, and for all $\theta, \xi \in C^{1,\infty}(\mathbb{R}^2;\mathbb{R}^2)$ we have*

$$E'(\Omega;\xi) = \int_\Gamma (\xi\cdot n)(\partial_n u)^2 \tag{4.19}$$

and

$$\begin{aligned} E''(\Omega;\theta,\xi) &= 2\int_\Gamma (\xi\cdot n)\nabla u'_\theta\cdot\nabla u + \int_\Gamma (\theta\cdot n)(\xi\cdot n)\big[(\partial_n+\mathcal{H})|\nabla u|^2\big] \\ &\quad + \int_\Gamma Z_{\theta,\xi}|\nabla u|^2, \end{aligned} \tag{4.20}$$

where $Z_{\theta,\xi}$ is given by (4.7). The function u'_θ is the shape derivative of the state function u and is solution to the following problem:

$$\begin{cases} -\Delta u'_\theta &= 0 & \text{in } \Omega, \\ u'_\theta &= -(\theta\cdot n)\partial_n u & \text{on } \Gamma. \end{cases} \tag{4.21}$$

The expression of the second order shape derivative E'' given by (4.20) may seem costly for numerical applications since one needs to compute u'_θ at every iteration. We shall see below how to deal with this difficulty.

Remark 4.2. Note that the first term in the right-hand side of (4.20) is bilinear and symmetric since $\nabla u = (\partial_n u)n$ (recall that $u_\Gamma = 0$) and so

$$\int_\Gamma (\xi \cdot n)\nabla u'_\theta \cdot \nabla u = \int_\Gamma (\xi \cdot n)\partial_n u \partial_n u'_\theta = -\int_\Gamma u'_\xi \partial_n u'_\theta = -\int_\Omega \nabla u'_\xi \cdot \nabla u'_\theta.$$

Before proceeding with the discrete optimization problem, we need the first and second order shape derivatives of the volume (area) constraint $V(\Omega) = \int_\Omega dx$. The following corollary is easily obtained by taking $f(x, y) = 1$ in (4.6).

Corollary 4.2. *Let $\Omega \in \mathcal{O}_3$. Then the area functional $V(\Omega)$ is twice shape differentiable, and for all $\theta, \xi \in C^{1,\infty}(\mathbb{R}^2; \mathbb{R}^2)$ we have*

$$V'(\Omega; \xi) = \int_\Gamma (\xi \cdot n), \tag{4.22}$$

and

$$V''(\Omega; \theta, \xi) = \int_\Gamma \mathcal{H}(\theta \cdot n)(\xi \cdot n) + \int_\Gamma Z_{\theta,\xi}, \tag{4.23}$$

where $Z_{\theta,\xi}$ is given by (4.7).

4.3.1. *Discretization of Newton's equation with volume constraint.* Let us now look at the shape optimization problem (4.18). We now have to deal with the volume constraint throughout the optimization process, and to do so we follow the results in [6, chapter 14]. In general, for a given constraint $c(\Omega)$, the right approach is to minimize the objective $E(\Omega)$ while keeping the constraint satisfied, which is called a primal-dual method. To describe this, according to the first-order optimality conditions, we know that when the constraint is qualified at a solution $\Omega^\star$, there exists a Lagrange multiplier $\lambda_* \in \mathbb{R}$ such that

$$\begin{cases} E'(\Omega^\star; \xi) + \lambda_* c'(\Omega^\star, \xi) & = 0, \quad \forall \xi, \\ c(\Omega^\star) = 0. \end{cases} \tag{4.24}$$

Thus, introducing the Lagrangian

$$L(\Omega_p, \lambda_p) = E(\Omega_p) + \lambda_p c(\Omega_p), \tag{4.25}$$

Newton's method defines a step in (Ω, μ) at (Ω_p, λ_p) by linearizing the system (4.24). One finds

$$\begin{pmatrix} L''_p & A_p^T \\ A_p & 0 \end{pmatrix} \begin{pmatrix} \theta_p \\ \mu_p \end{pmatrix} = -\begin{pmatrix} L'_p \\ c_p \end{pmatrix}, \tag{4.26}$$

where $L''_p := L''(\Omega_p; \theta, \xi)$ and $L'_p := L'(\Omega_p; \xi)$ are the first and second order shape derivatives of the Lagrangian L at Ω_p (for a fixed λ_p), $c_p = c(\Omega_p)$ and $A_p := c'(\Omega_p; \xi)$ is the shape derivative of the constraint. Given a solution (θ_p, μ_p) to (4.26), Newton's method defines the next iterate $(\Omega_{p+1}, \lambda_{p+1})$ by

$$\Omega_{p+1} = (I + \theta_p)(\Omega_p) \qquad \text{and} \qquad \lambda_{p+1} = \lambda_p + \mu_p. \tag{4.27}$$

We then proceed to build the left hand side of (4.26) using the discretization described earlier in Section 4.2.1. Once again, we seek a continuous piecewise linear vector field θ_h as in (4.10). By choosing the discrete normal vector field $\xi_h(x) =$

$\varphi_i(x)n_h(\mathbf{x}_i)$ where φ_i is the hat function at $\mathbf{x}_i$, we obtain from (4.22) that A_p is the row vector with entries

$$A_p[i] = \int_{\Gamma_h} \varphi_i(x)n_h(\mathbf{x}_i)\cdot n_h(x)dx \approx \frac{h_i^- + h_i^+}{2} n_h(\mathbf{x}_i)\cdot n_h(\mathbf{x}_i) = \frac{h_i^- + h_i^+}{2}.$$

As previously, we used the trapezoidal rule to evaluate the integral above. Moreover, for each vertex $\mathbf{x}_i$, h_i^+ and h_i^- are the lengths of the edges $[\mathbf{x}_{i-1}, \mathbf{x}_i]$ and $[\mathbf{x}_i, \mathbf{x}_{i+1}]$ arriving at $\mathbf{x}_i$.

The matrix $L_p^{''}$ is the Hessian of the Lagrangian L. Using the expressions (4.20) and (4.23), we obtain that $L_p^{''}$ is a matrix of size $n_{be}\times n_{be}$ with entries given by

$$\begin{aligned} L_p^{''}[i,j] = &\int_{\Gamma_h} 2(\varphi_i(x)n_h(\mathbf{x}_i)\cdot n_h(x))\nabla u_{n_h^j}^{h'}(x)\cdot\nabla u_h(x) \\ &+ \int_{\Gamma_h} (\varphi_i(x)n_h(\mathbf{x}_i)\cdot n_h(x))(\varphi_j(x)n_h(\mathbf{x}_j)\cdot n_h(x))(\partial_{n_h}+\kappa(x))|\nabla u_h(x)|^2 \\ &+ \lambda\int_{\Gamma_h} (\varphi_i(x)n_h(\mathbf{x}_i)\cdot n_h(x))(\varphi_j(x)n_h(\mathbf{x}_j)\cdot n_h(x))\kappa(x)dx. \end{aligned}$$

In this expression, u_h is the discrete $\mathbb{P}_1$ solution to the state equation (4.17) and $u_{n_h^j}^{h'}$ is the discrete ($\mathbb{P}_1$) solution to problem (4.21) with $\theta(x) = \varphi_j(x)n_h(\mathbf{x}_j)$. Using a trapezoidale rule to evaluate the integrals, we obtain

$$\begin{aligned} L_p^{''}[i,j] \;=\; &\left(\frac{h_i^- + h_i^+}{2}\right)\left(2\nabla u_{n_h^j}^{h'}(\mathbf{x}_i)\cdot\nabla u_h(\mathbf{x}_i)\right) \\ &+\delta_{ij}\left(\frac{h_i^- + h_i^+}{2}\right)\left((\partial_{n_h}+\kappa(\mathbf{x}_i))|\nabla u_h(\mathbf{x}_i)|^2 + \lambda\kappa(\mathbf{x}_i)\right). \end{aligned}$$

Owing to the term δ_{ij}, the matrix $L_p^{''}$ is diagonal, except for the first term involving $\nabla u_{n_h^j}^{h'}(\mathbf{x}_i)$ which is nonlocal. In practice, we only keep the diagonal terms in $L_p^{''}$, leading to a *quasi-Newton method*.

Going back to the continuous problem (4.21), we have $u'_\theta = (\theta\cdot n)\partial_n u$. In particular, tor $\theta = n$, this gives $u'_n(\mathbf{x}_i) = \partial_n u(\mathbf{x}_i)$. Thus, we can write

$$\begin{aligned} \nabla u'_n &= \nabla(\nabla u\cdot n) \\ &= D^2u\, n + Dn.\nabla u \\ &= D^2u.n + \partial_n u\, Dn.n \qquad (\nabla_\Gamma u = 0) \\ &= D^2u.n \qquad (Dn.n = 0 \text{ since } n \text{ is unitary on } \Gamma). \end{aligned}$$

This allows us to rewrite $\nabla u_{n_i}^{h'}(\mathbf{x}_i) = D^2u_h(\mathbf{x}_i).n_h(\mathbf{x}_i)$. This could seem problematic at first sight. Indeed, u_h is only $\mathbb{P}_1$ and thus $\nabla u_h = (\partial_x u_h, \partial_y u_h)^T$ is only a $\mathbb{P}_0$ function on $\mathcal{T}_h$, i.e., it is constant on each triangle T_i. We thus seek to lift this function as a $\mathbb{P}_1$ function. The easiest way to do so is by interpolation, but our experiments show that the most accurate way to do this is through a least-squares matching of the gradient ∇u_h on the vertices $\mathbf{x}_i$ of Γ. This is described in detail in Appendix A.

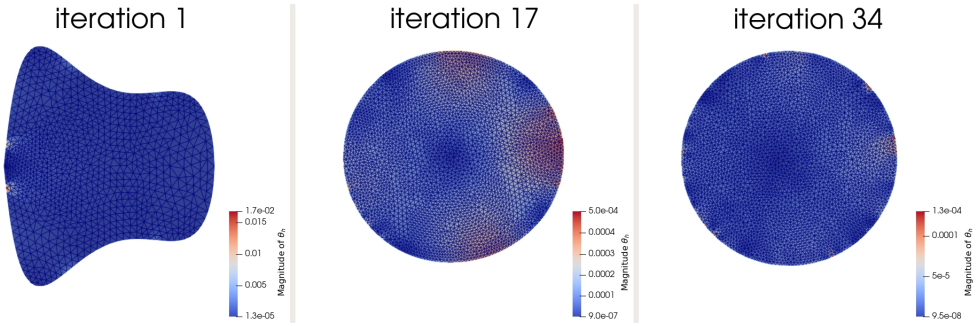

FIGURE 13. The starting shape (left), a nearly optimal shape (middle) and the best shape (right), with the magnitude of the descent direction θ for the minimization of the Dirichlet energy.

In particular, we define the operator ∇^h (see (A.6)),

$$\begin{cases} \nabla^h : \mathcal{V}_h \Longrightarrow \mathcal{V}_h \times \mathcal{V}_h \\ \varphi_h \mapsto \nabla^h \varphi_h \approx \nabla \varphi_h. \end{cases}$$

Not only is this an accurate way of approximating the gradient, but its (almost) local character also allows us to cut down on unnecessary computations on the interior of the domain Ω_h. Indeed, $L_p^{''}$ is only defined on the boundary Γ_h, so we only need the values of the gradient as a $\mathbb{P}_1$ function on a neighborhood of the boundary vertices $\mathbf{x}_i$. Notice also that this solves the issue of computing the term $\partial_n\big(|\nabla u|^2\big)$, since we can compute

$$\partial_{n_h}\big(|\nabla u_h|^2\big)(\mathbf{x}_i) = \nabla_i^h\big(|\nabla^h u_h|^2\big) \cdot n_h(\mathbf{x}_i),$$

where, for a continuous function g, $\nabla_i^h g = \nabla^h g(\mathbf{x}_i)$. We stress that the operator $\nabla^h : C^0(\overline{\Omega_h}) \to \mathcal{V}_h \times \mathcal{V}_h$ is actually defined for any continuous function. Here, it applies to the continuous $\mathbb{P}_2$ function $|\nabla^h u_h|^2$.

Ultimately, the diagonal entries of the Hessian $L_p^{''}$ and the entries of $L_p^{'}$ read

$$L_p^{''}[i,i] = 2\nabla_i^h\big(\nabla^h u_h\big).n_h(\mathbf{x}_i) \cdot \nabla_i^h u_h + \nabla_i^h\big(|\nabla^h u_h|^2\big) \cdot n_h(\mathbf{x}_i) + \kappa(\mathbf{x}_i)\big(\lambda + |\nabla_i^h u_h|^2\big) \tag{4.28}$$

$$L_p^{'}[i] = \lambda + \big(\nabla_i^h u_h \cdot n_h(\mathbf{x}_i)\big)^2. \tag{4.29}$$

We have divided these entries by $(h_i^+ + h_i^-)/2$ which is common to both sides.

4.3.2. *Numerical results.* In this section, we test our discretization to compute the optimal shape $\Omega^\star$ for minimizing the Dirichlet energy (4.16) under volume (area, since $d = 2$) constraint $|\Omega| = 0.4$. Recall that the optimal shape in this case is a disc of area 0.4. Starting from a random guess, we successively compute a descent direction by solving (4.26) that we use to move the shape with a constant step $t = 1$ as defined in (4.27). We also compare Newton's method with an augmented Lagrangian method [27].

As stated in the introduction of [11], the tuning of the penalty parameters for the augmented Lagrangian is strongly case-dependent. Thus, we perform a series of tests with different penalty parameters and time steps and we retain the fastest in order to compare it with Newton's algorithm. We take a constant time step

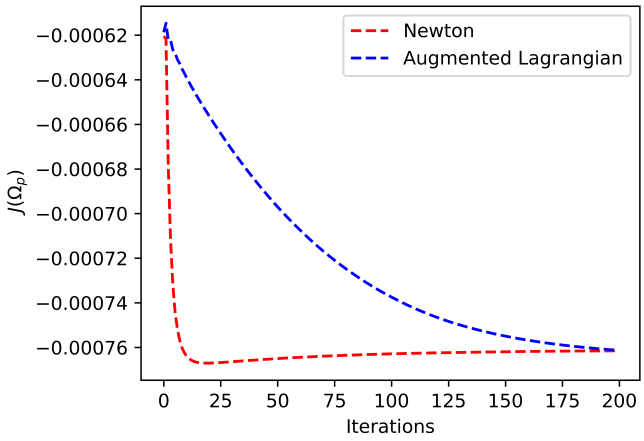

FIGURE 14. Convergence of the Dirichlet energy

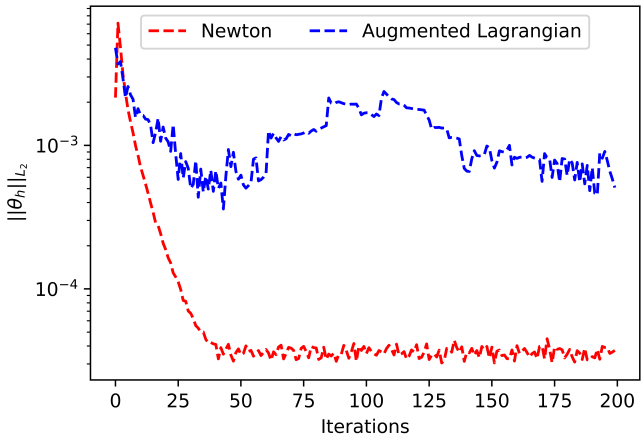

FIGURE 15. The L_2 norm of the descent direction θ_h at every iteration of the minimization process.

$t = 0.4$ and a quadratic penalty parameter $\mu < 10$ for the augmented Lagrangian algorithm. Figure 13 shows the starting shape and the optimal shape. In both cases, the algorithm converges to a ball, as expected.

As seen in Figures 14 and 15, Newton's algorithm is remarkably fast and converges in about 20 iterations. In contrast, the augmented Lagrangian takes 10 times longer to converge. Figure 16 shows that the volume constraint is reasonably satisfied during the whole process.

5. Optimal hull with optimized support

5.1. **Theoretical results.** We introduce a "bounding box", namely a bounded and connected open subset Q of the upper half plane $\{(x, z) \in \mathbb{R}^2 \ : \ z > 0\}$. We assume that Q has a Lipschitz boundary ∂Q such that $\partial Q \cap (\mathbb{R} \times \{0\})$ is a segment of the

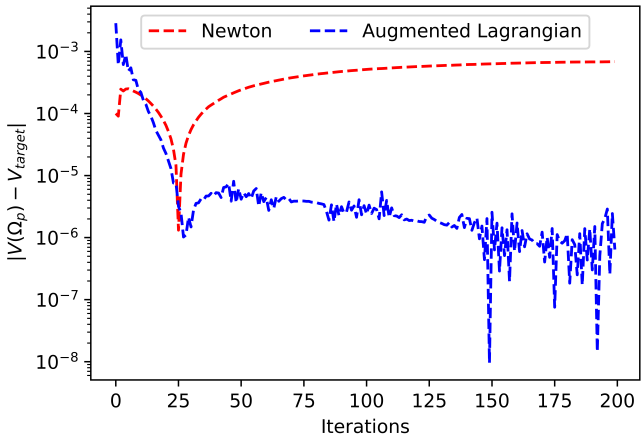

FIGURE 16. Convergence of the area constraint $|V(\Omega_p) - V_{target}|$.

x-axis (possibly empty). We denote by ∂Q_N the (relative) interior of this segment and $\partial Q_0 = \partial D \setminus \partial Q_N$.

For instance, Q can be a half disc with a large radius and centered on the x-axis or a rectangle with one side of its boundary included in the x-axis.

We introduce the Sobolev space

$$H(Q) = \left\{ u \in H^1(Q) \ : u = 0 \text{ on } \partial Q_0 \text{ in the sense of trace} \right\},$$

equipped with the H^1 norm. For each function $u \in H^1(Q)$, we denote its support by

$$D_u = \{(x, z) \in Q \ : \ u(x, z) \neq 0\}.$$

The set D_u is unique up to a set of zero Lebesgue-measure and its area $|D_u|$ does not depend on the choice of the representative of u.

Let $a \in (0, |Q|)$ (an area) and $\mathcal{V} > 0$ (a volume). Following [8], we introduce the set

$$C_{\mathcal{V},a}(Q) = \left\{ u \in H(Q) \ : \ \int_Q u \, dxdz = \mathcal{V} \text{ and } |D_u| \leq a \right\}.$$

The set $C_{\mathcal{V},a}$ is a closed subset of $H(Q)$.

As in Section 3.1, we assume that the Kelvin wave number is a random variable $\nu : \Omega \to \mathbb{R}$ whose probability distribution has a compact support in $(0, +\infty)$.

For $u \in H(Q)$, the functional is

$$\mathcal{J}(u) = \mathbb{E}\left[\tilde{h}(\nu) \left(2a + J_0(u) + \frac{1}{C_F} J_{wave}(u, \nu) \right) \right],$$

where $\tilde{h} : (0, +\infty) \to (0, +\infty)$ is a continuous function which depends on the fixed parameters ρ, g and C_F. The functions J_0 and J_{wave} are defined as previously, except that the integration on D is replaced by an integration on Q. That is, we have

$$J_0(u) = \int_Q |\nabla u|^2 dxdz$$

and

$$J_{wave}(u,\alpha) = \frac{8\alpha^4}{\pi}\int_1^\infty |T(u,\alpha,\lambda)|^2 \frac{\lambda^4}{\sqrt{\lambda^2-1}} d\lambda,$$

where T is defined for all $u \in H(Q)$, $\alpha > 0$ and $\lambda > 0$ by

$$T(u,\alpha,\lambda) = \int_Q u(x,z) e^{-i\lambda\alpha x} e^{-\lambda^2\alpha z} dxdz.$$

We recall that the bounding box Q and the function $\tilde{h}$ are given, and that the positive parameters ρ, g, C_F, a and $\mathcal{V}$ are fixed. The problem reads:

$$\text{Find } u^\star \in C_{\mathcal{V},a}(Q) \text{ such that } \mathcal{J}(u^\star) = \min_{u \in C_{\mathcal{V},a}(Q)} \mathcal{J}(u). \tag{5.1}$$

The support $D_{u^\star}$ of $u^\star$ will be called on *optimal domain*. We note that $u^\star$ is generally not unique, because $\mathcal{J}$ is invariant with respect to translations along the x-axis. Moreover, the set $C_{\mathcal{V},a}(Q)$ is not convex, so that an optimal domain $D_{u^\star}$ is not necessarily unique up to translations along the x-axis. We have:

Theorem 5.1. *Problem* (5.1) *has at least one solution* $u^\star$.

Proof. Let $(u_n)_n$ be a minimizing sequence in $C_{\mathcal{V},a}(Q)$. We have

$$\mathcal{J}(u_n) = 2a\mathbb{E}\left[\tilde{h}(\nu)\right] + \mathbb{E}\left[\tilde{h}(\nu)\right] J_0(u_n) + \frac{1}{C_F}\mathbb{E}\left[\tilde{h}(\nu) J_{wave}(u_n,\nu)\right],$$

and each term in the sum above is nonnegative. This implies that the sequence $(J_0(u_n))_n$ is bounded, and so (u_n) is bounded in $H^1(Q)$, by the Poincaré inequality. Let $q' > 5$. By compactness, there is a subsequence still denoted by (u_n) and $u^\star \in H(Q)$ such that (u_n) converges to $u^\star$ weakly in $H(Q)$, strongly in $L^{q'}(Q)$ and a.e. in Q. By Fatou's lemma, we have

$$|D_{u^\star}| = \int_Q 1_{u^\star} dxdz \le \liminf_n \int_Q 1_{u_n} dxdz = |D_{u_n}| \le a,$$

where 1_v denotes the characteristic function of a function $v \in H(Q)$. Thus, $u^\star$ belongs to $C_{\mathcal{V},a}(Q)$. By lower semi-continuity of J_0, we have

$$J_0(u^\star) \le \liminf_n J_0(u_n). \tag{5.2}$$

We may apply Proposition 3.4 with the set D replaced by Q. Since (u_n) converges strongly in $L^{q'}(Q)$, we have

$$\mathbb{E}\left[\tilde{h}(\nu) J_{wave}(u_n,\nu)\right] \to \mathbb{E}\left[\tilde{h}(\nu) J_{wave}(u^\star,\nu)\right]. \tag{5.3}$$

The relations (5.2) and (5.3) show that

$$\mathcal{J}(u^\star) \le \liminf_n \mathcal{J}(u_n).$$

Since (u_n) is a minimizing sequence, $u^\star$ is a solution to problem (5.1). □

5.2. **Numerical simulations.** We want to compute the optimal shape for minimizing the expectation of the total water resistance under area constraint. That is, for a given area $a > 0$, we wish to solve numerically the following problem,

$$\min_{|D|=a} \mathcal{J}(D), \tag{5.4}$$

among bounded open subsets D of the upper half plane which are admissible. As a shortcut, we have denoted by $\mathcal{J}$ the functional

$$D \mapsto \mathcal{J}_D(u_D^\star),$$

where $\mathcal{J}_D$ is defined by (3.8) with the choice (3.17) for $\tilde{h}$ and $u_D^\star$ is the solution to the minimization problem (3.18).

By (3.22), solving (5.4) is the same as solving

$$\min_{|D|=a} \tilde{\mathcal{J}}(D) \tag{5.5}$$

where

$$\tilde{\mathcal{J}}(D) = \int_D |\nabla u_D^\star|^2 + \frac{1}{C_F \mathbb{E}[\tilde{h}(\nu)]} \int_{D\times D} H_\nu(x,z,x',z') u_D^\star(x,z) u_D^\star(x',z'),$$

and $u_D^\star$ is the solution to the boundary value problem (cf. (3.16))

$$\begin{cases} -\Delta u(x,z) + \dfrac{1}{C_F \mathbb{E}\left[\tilde{h}(\nu)\right]} \displaystyle\int_{D\times D} H_\nu(x,z,x',z') u(x',z') dx'dz' = C, \ \forall (x,z) \in D, \\ \int_D u \, dxdz = \mathcal{V}, \\ u = 0 \text{ on } \Gamma_0, \\ \dfrac{\partial u}{\partial n} = 0 \text{ on } \Gamma_N. \end{cases} \tag{5.6}$$

Throughout Section 5.2, D is a simply connected and bounded open subset of the upper half plane with Lipschitz boundary. We assume that $\partial D \cap (\mathbb{R} \times \{0\})$ is a segment and we denote by Γ_N the relative interior of this segment. We also assume that the curve $\Gamma_0 = \partial D \setminus \Gamma_N$ is of class C^3 (see Figure 2).

5.2.1. *Shape derivatives.* The shape sensitivity analysis of $\tilde{\mathcal{J}}$ is very similar to the case of the Dirichlet energy, assuming enough regularity. The result is very similar to Theorem 4.1 (up to the minus sign). The calculations for a smooth domain and a smooth kernel are given in [38, Section 8.3] (see also [19]).

In our case, we will use the following expressions. Let $\mathbb{R}^2_+ = \mathbb{R} \times [0, +\infty)$ denote the closed upper half plane. For all $\theta, \xi \in C^{1,\infty}(\mathbb{R}^2_+; \mathbb{R}^2)$ such that $\theta \cdot n = 0$ and $\xi \cdot n = 0$ on the x-axis, we have

$$\tilde{\mathcal{J}}'(D;\xi) = -\int_{\Gamma_0} (\xi \cdot n)(\partial_n u)^2 \tag{5.7}$$

and

$$\begin{aligned} \tilde{\mathcal{J}}''(D;\theta,\xi) = &-2\int_{\Gamma_0} (\xi\cdot n) \nabla u'_\theta \cdot \nabla u - \int_{\Gamma_0} (\theta\cdot n)(\xi\cdot n)\big[(\partial_n + \mathcal{H})|\nabla u|^2\big] \\ &- \int_{\Gamma_0} Z_{\theta,\xi} |\nabla u|^2 \end{aligned} \tag{5.8}$$

where u solves (5.6), $Z_{\theta,\xi}$ is given by (4.7) and u'_θ is solution to the following problem:

$$\begin{cases} -\Delta u'_\theta + \dfrac{1}{C_F \mathbb{E}\left[\tilde{h}(\nu)\right]} \displaystyle\int_{D\times D} H_\nu(\cdot,\cdot,x',z') u'_\theta(x',z') dx'dz' = \tilde{C} & \text{in } D, \\ \int_D u'_\theta \, dxdz = 0, \\ u'_\theta = -(\theta \cdot n)\partial_n u \text{ on } \Gamma_0, \\ \dfrac{\partial u'_\theta}{\partial n} = 0 \text{ on } \Gamma_N. \end{cases} \tag{5.9}$$

The same discretization as in Section 4.3.1 can be used to apply Newton's algorithm to the set functional $\tilde{\mathcal{J}}$, assuming enough regularity both on the domain D and the kernel H_ν. Even in situations where these regularity constraints are not satisfied, for example when the domain contains corners or when the kernel is not regular enough, the discretization (4.26) provides enough flexibility to get around these issues, as explained below in Section 5.2.2.

5.2.2. *Tips for Newton's algorithm.* In this section, we seek to compute the optimal shape $D^\star$ by Newton's method discretized as in Section 4.3. There are two main obstructions to regularity in the expression of the second order shape derivative (5.8). First, Michell's kernel H_ν does not belong to $L^2(D)$. It is only in $L^{\frac{5}{4}-\varepsilon}(D)$ for all $\varepsilon > 0$ small enough, as proved in [8]. Second, the boundary expression of the second order derivative given by (5.8) is only given for domains D that are at least C^3 (with $\Gamma_N = \emptyset$ and $\Gamma_0 = \partial D$) while D here is only C^3 on each boundary Γ_0 and Γ_N. We shall always have two corners at the intersection of the boundaries.

These regularity issues make it a priori difficult to attempt a second order shape optmization method. Since the boundary expression of the second order shape derivative is ill-defined, one could then try to find a different expression that takes into account the irregularity of the boundary. This is extensively studied in [23] for the case of the Dirichlet energy and volume functional, and the interested reader can find in it expressions for the second order derivative given for domains that are only Lipschitz.

In our case, it turns out that the discretization (4.13) gives enough flexibility to get around these issues when building the discrete Hessian matrix. Indeed, the discrete Hessian shall only be constructed on the vertices of the boundary Γ_0. Since our discretization is strictly dependent on the discrete normal $n_h(\mathbf{x}_i)$ on a vertex $\mathbf{x}_i$, in order to remain consistent, we exclude the vertices $\mathbf{x}_i$ with singularities (in this case, the first and last vertex of Γ_0) when building the discrete Hessian. The value $\theta_h(\mathbf{x}_i)$ on each one of these two vertices is then obtained by keeping the horizontal component of the neighboring value $\theta_h(\mathbf{x}_{i+1})$ computed on Γ_0. In this way, the constraint on Γ_N is preserved, namely

$$\theta_h(\mathbf{x}_i) \cdot n_h(\mathbf{x}_i) = 0 \qquad \text{on } \Gamma_N.$$

Finally, while theoretically the solution u is not in $H^2(D)$, we still can discretize quantities such as $\nabla^2 u$ using numerical gradients, specifically the least-squares gradient defined in Appendix A. This least-square gradient will enjoy higher regularity and ensures that the resulting discrete Hessian matrix is well conditioned.

These are all the tips that were used to help Newton's algorithm to converge on an irregular domain with an irregular solution, and the results are given in the next

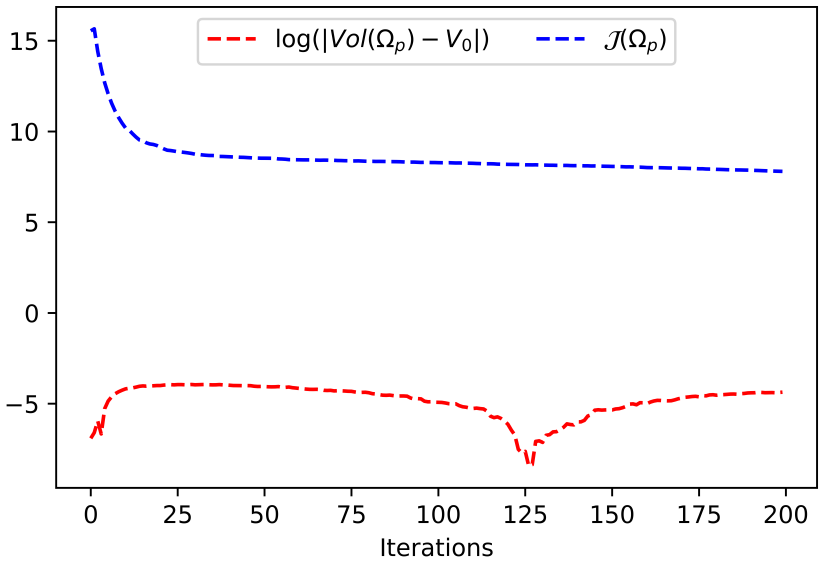

FIGURE 17. Convergence results for the expectation of the total resistance and for the volume constraint using Newton's algorithm.

section. While these tips seems complicated and a little bit technical, they are easy to implement for a trained `FreeFem++` user [18].

5.2.3. *Numerical results.* For all our numerical simulations, the initial domain D_0 is taken as the half-ellipse, centered at the origin of length 2.2 m and draft 0.3 m. The area of D_0 is therefore $a = 0.518\,\mathrm{m}^2$. The volume of the hull is fixed at $\mathcal{V} = 0.06\,\mathrm{m}^3$, and we consider a uniform probability distribution of the Kelvin wave number $\alpha \in [\nu_{\min}, \nu_{\max}]$. The parameters ρ, g, C_F are as in (3.20) and $\tilde{h}$ is defined by (3.17).

For the sake of comparison with the results in [8], we introduce the area Froude number

$$F_r^2 = \frac{1}{\alpha\sqrt{a}} = \frac{V^2}{g\sqrt{a}},$$

where $a = 0.518\ \mathrm{m}^2$ is the area of D. The bounds $\nu_{\min}$ and $\nu_{\max}$ are computed as

$$\nu_{\min} = \frac{1}{\sqrt{a} Fr_{\max}^2} \quad \text{and} \quad \nu_{\max} = \frac{1}{\sqrt{a} Fr_{\min}^2}.$$

For our numerical results, we focus on the Froude interval $[0.6, 1.0]$. This is the range of speed where it is most interesting to have a bulb in order to minimize the total ship resistance, as seen in [9].

We first compute the optimal domain $D^\star$ which minimizes the expectation of the total water resistance $\tilde{\mathcal{J}}$. Figure 18 (bottom) shows the optimal domain computed with Newton's algorithm. The corresponding optimal hull $u^\star$ is represented in Figure 19 (bottom). The convergence of the algorithm is given in Figure 17. We can see that Newton's algorithm converges very fast without the need of a line search, since a constant time step $t = 1$ was used throughout the optimisation process.

As a comparison, we have also computed the domain which minimizes the total resistance for the mean Kelvin number $\alpha = \mathbb{E}(\nu)$ related to the Froude number

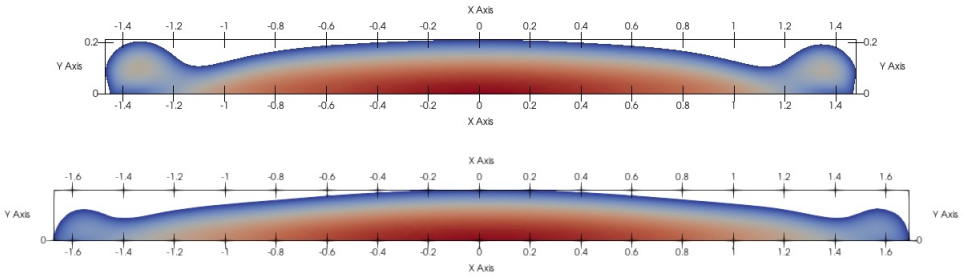

FIGURE 18. The optimal domains for minimizing the total resistance at $Fr = 0.73$ (top) and for minimizing the expectation of the total resistance for $Fr \in [0.6, 1]$ with ν uniform (bottom).

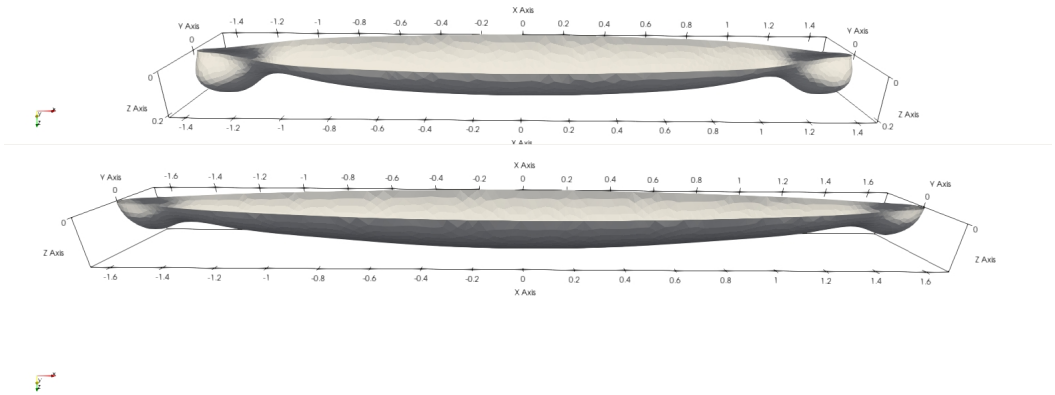

FIGURE 19. The optimal hulls for minimizing the total water resistance at $Fr = 0.73$ ($\bar{u}$, top) and for minimizing the expectation of the total resistance for $Fr \in [0.6, 1]$ with ν uniform ($u^\star$, bottom).

$Fr = 0.73$ (Figure 18, top) and the corresponding optimal hull $\bar{u}$ (Figure 19, top). We use the same algorithm (Newton's method), except that the averaged kernel H_ν is replaced by Michell's kernel $\tilde{h}(\alpha)k_\alpha$ (see Remark 3.2), so the computation is less costly.

The two optimal domains and the corresponding hulls $u^\star$ and $\bar{u}$ are different: the bulbous bow is more pronounced for $\bar{u}$ than for $u^\star$. In contrast u^* is longer than $\bar{u}$ since it takes into account higher Froude numbers. We refer here to [9, Section 7] where it is seen that the length of the optimal domain increases with the Froude number.

Despite these remarkable geometric differences, we can see in Figure 20 that the total resistance is very similar for both hulls on the whole interval $[0.6, 1.0]$. The expectation of the total resistance is equal to 26.3 N for $u^\star$ and it is equal to 27.1 N for $\bar{u}$. We note however that $\bar{u}$ is optimal for $\alpha = \mathbb{E}(\nu)$ and slightly better for Froude

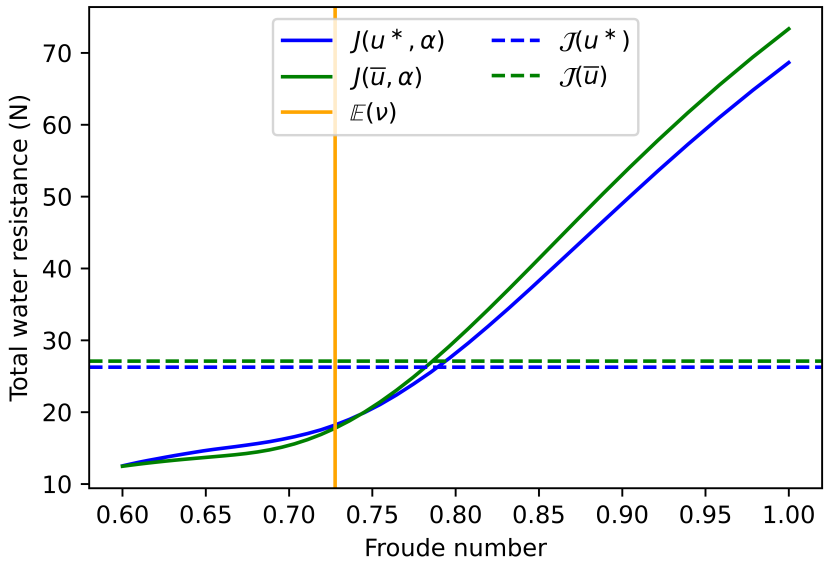

FIGURE 20. The total water resistance of the two hulls

number less than 0.75, while $u^\star$ is better on the rest of the interval. Both hulls perform much better than a Wigley hull.

As a comparison, we have performed computations for the Wigley w defined by the function (3.28) and the parameters $L = 2\,\mathrm{m}$, $T = 0.255\,\mathrm{m}$ and $B = 0.7272\,\mathrm{m}$. For this choice, we have $a = 0.51\,\mathrm{m}^2$ and $\mathcal{V} = 0.06\,\mathrm{m}^3$ (see (3.29)). The total resistance of w increases from 27.4 N for $Fr = 0.6$ to 211.2 N for $Fr = 1.0$. Its expectation is equal to 113.2 N.

APPENDIX A. GRADIENT OF A PIECEWISE LINEAR FUNCTION

In this appendix, we define a continuous gradient of a $\mathbb{P}_1$ function. This is used in our shape optimization algorithms.

For a domain D in $\mathbb{R}^2$ with a Lipschitz boundary Γ, we denote by $\mathcal{T}_h$ a conforming triangulation of D with typical mesh size h. The triangulation $\mathcal{T}_h$ contains n_t triangles T_i. The approximation of the domain D is the polygonal domain $D_h = \cup_{i=1}^{n_t} T_i$ and we denote by Γ_h the boundary of D_h.

The space of continous piecewise linear ($\mathbb{P}_1$) functions is denoted by $\mathcal{V}_h$, namely

$$\mathcal{V}_h = \left\{ u \in C(D_h, \mathbb{R}) \middle| \forall\, T_i \in \mathcal{T}_h,\ u_{|T_i} \in \mathbb{P}_1 \right\},$$

where $\mathbb{P}_1$ is the space of polynomials of degree less than or equal to 1.

If u belongs to $\mathcal{V}_h$, then the gradient ∇u is only a discontinuous $\mathbb{P}_0$ function on $\mathcal{T}_h$. i.e. it is equal to a constant value α_i on each triangle T_i. In many cases, we seek to lift this gradient to a $\mathbb{P}_1$ function defined on the vertices of $\mathcal{T}_h$ through a stable approximation.

Let $\mathbf{x}_0$ be a vertex of $\mathcal{T}_h$ and denote by $\mathbf{x}_1, \ldots, \mathbf{x}_n$ the neighboring vertices as given in Figure 21. For a smooth function $f : \mathbb{R}^2 \to \mathbb{R}$, we have the following Taylor

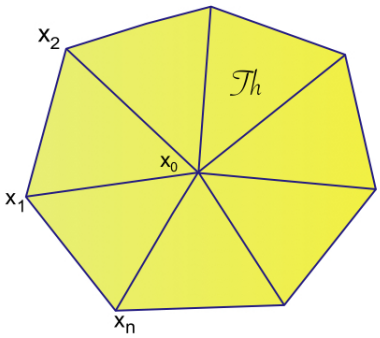

FIGURE 21. Neighborhood of a vertex $\mathbf{x}_0$ in a mesh $\mathcal{T}_h$.

expansion around $\mathbf{x}_0$,

$$f(\mathbf{x}_i) \approx f(\mathbf{x}_0) + \nabla f(\mathbf{x}_0) \cdot (\mathbf{x}_i - \mathbf{x}_0), \quad \text{for } i = 1, \dots, n. \tag{A.1}$$

Then following [13], a good approximation of the gradient ∇u of our piecewise linear function u may be obtained by mimicking the expansion (A.1) for all $i = 1, \dots, n$. That is, we approximate ∇u by a vector $b = (b_1, b_2)$ solution to

$$Ab = c, \tag{A.2}$$

where A and c are the $n \times 2$ matrix and n-dimensional vector given by:

$$A = \begin{pmatrix} \mathrm{x}_1^1 - \mathrm{x}_0^1 & \mathrm{x}_1^2 - \mathrm{x}_0^2 \\ \mathrm{x}_2^1 - \mathrm{x}_0^1 & \mathrm{x}_2^2 - \mathrm{x}_0^2 \\ \vdots & \vdots \\ \mathrm{x}_n^1 - \mathrm{x}_0^1 & \mathrm{x}_n^2 - \mathrm{x}_0^2 \end{pmatrix} \qquad \text{and} \qquad c = \begin{pmatrix} u(\mathbf{x}_1) - u(\mathbf{x}_0) \\ u(\mathbf{x}_2) - u(\mathbf{x}_0) \\ \vdots \\ u(\mathbf{x}_n) - u(\mathbf{x}_0) \end{pmatrix}. \tag{A.3}$$

However, problem (A.2) is clearly overdetermined, and in practice we search b as a solution to the least-square problem

$$A^T A b = A^T c, \tag{A.4}$$

where A^T is the transpose of A. In (A.4), $A^T c$ is a two-dimensional vector and $A^T A$ is the 2×2 matrix defined by

$$A^T A = \begin{pmatrix} \sum_{i=1}^n (\mathrm{x}_i^1 - \mathrm{x}_0^1)^2 & \sum_{i=1}^n (\mathrm{x}_i^1 - \mathrm{x}_0^1)(\mathrm{x}_i^2 - \mathrm{x}_0^2) \\ \sum_{i=1}^n (\mathrm{x}_i^1 - \mathrm{x}_0^1)(\mathrm{x}_i^2 - \mathrm{x}_0^2) & \sum_{i=1}^n (\mathrm{x}_i^2 - \mathrm{x}_0^2)^2 \end{pmatrix}.$$

The matrix $A^T A$ is invertible since $det(A^T A) > 0$ as a consequence of the Cauchy-Schwarz inequality.

By repeating the procedure above, we obtain a value for the gradient of u at every vertex of the triangulation $\mathcal{T}_h$, and by linear interpolation, a function (v_h, w_h) in $\mathcal{V}_h \times \mathcal{V}_h$. This approach for approximating the gradient ∇u as a continuous $\mathbb{P}_1$ function is pretty robust in practice. Unfortunately, it may still be affected by numerical errors, and this is a reason why it is often recommended to smooth the resulting quantities.

To this end, it is common practice to use the screened Poisson equation, i.e. for a $\mathbb{P}_1$ function $\psi \in \mathcal{V}_h$, we trade ψ for the solution $\tilde{\psi} \in \mathcal{V}_h$ to the following variational problem:

$$\forall\, \varphi_h \in \mathcal{V}_h, \quad \int_{D_h} (\varepsilon^2 \nabla\tilde{\psi} \cdot \nabla\varphi_h + \tilde{\psi}\varphi_h) dx = \int_{D_h} \psi\varphi_h dx, \tag{A.5}$$

where ε is chosen of the order of mesh size, that is, $\varepsilon \approx h$.

Summing up, for a function $u \in \mathcal{V}_h$, we define its continuous $\mathbb{P}_1$ gradient as

$$\nabla^h u = (\tilde{v}_h, \tilde{w}_h), \tag{A.6}$$

where $\tilde{v}_h \in \mathcal{V}_h$ and $\tilde{w}_h \in \mathcal{V}_h$ are obtained by smoothing v_h and w_h respectively, and $(v_h, w_h) \in \mathcal{V}_h \times \mathcal{V}_h$ is obtained at each vertex of the triangulation by the local least square problem described above. We note that this definition of $\nabla^h u$ makes senses for any continuous function $u \in C^0(\overline{D_h})$.

References

[1] R. A. Adams. *Sobolev spaces*. Pure and Applied Mathematics, Vol. 65. Academic Press [Harcourt Brace Jovanovich, Publishers], New York-London, 1975.

[2] A. Ahmad Ali, E. Ullmann, and M. Hinze. Multilevel Monte Carlo analysis for optimal control of elliptic PDEs with random coefficients. *SIAM/ASA J. Uncertain. Quantif.*, 5(1):466–492, 2017.

[3] G. Allaire, E. Cancès, and J.-L. Vié. Second-order shape derivatives along normal trajectories, governed by Hamilton-Jacobi equations. *Struct. Multidiscip. Optim.*, 54(5):1245–1266, 2016.

[4] G. Allaire, C. Dapogny, and F. Jouve. Shape and topology optimization. In *Geometric partial differential equations. Part II*, volume 22 of *Handb. Numer. Anal.*, pages 1–132. Elsevier/North-Holland, Amsterdam, 2021.

[5] L. Birk. *Fundamentals of ship hydrodynamics: Fluid mechanics, ship resistance and propulsion*. John Wiley & Sons, 2019.

[6] J. Bonnans, J. C. Gilbert, C. Lemaréchal, and C. Sagastizbal. *Numerical optimization*. Universitext. Springer-Verlag, Berlin, second edition, 2006.

[7] D. Bucur. Do optimal shapes exist? *Milan J. Math.*, 75:379–398, 2007.

[8] J. Dambrine and M. Pierre. Regularity of optimal ship forms based on Michell's wave resistance. *Appl. Math. Optim.*, 82(1):23–62, 2020.

[9] J. Dambrine and M. Pierre. Continuity with respect to the speed for optimal ship forms based on Michell's formula. *Math. Control Relat. Fields*, 13(1):63–93, 2023.

[10] J. Dambrine, M. Pierre, and G. Rousseaux. A theoretical and numerical determination of optimal ship forms based on Michell's wave resistance. *ESAIM Control Optim. Calc. Var.*, 22(1):88–111, 2016.

[11] Feppon, F., Allaire, G., and Dapogny, C. Null space gradient flows for constrained optimization with applications to shape optimization. *ESAIM: COCV*, 26(90):45, 2020.

[12] L. D. Ferreiro. The social history of the bulbous bow. *Technology and Culture*, 52(2):335–359, 2011.

[13] P. Frey and P.-L. George. *Mesh generation*. ISTE, London; John Wiley & Sons, Inc., Hoboken, NJ, second edition, 2008.

[14] A. S. Gotman. Study of Michell's integral and influence of viscosity and ship hull form on wave resistance. *Oceanic Engineering International*, 6:74–115, 2002.

[15] P. Grisvard. *Elliptic problems in nonsmooth domains*, volume 69 of *Classics in Applied Mathematics*. Society for Industrial and Applied Mathematics (SIAM), Philadelphia, PA, 2011.

[16] J. Hadamard. *Œuvres de Jacques Hadamard. Tomes I, II, III, IV*. Éditions du Centre National de la Recherche Scientifique, Paris, 1968.

[17] H. Harbrecht. A Newton method for Bernoulli's free boundary problem in three dimensions. *Computing*, 82(1):11–30, 2008.

[18] F. Hecht. New development in FreeFem++. *J. Numer. Math.*, 20(3-4):251–265, 2012.

[19] A. Henrot and M. Pierre. *Shape variation and optimization*, volume 28 of *EMS Tracts in Mathematics*. European Mathematical Society (EMS), Zürich, 2018.
[20] C.-C. Hsiung and S. Dong. Optimal ship forms for minimum total resistance. *J. Ship Res.*, 28(3):163–172, 1984.
[21] M. G. Krein and V. G. Sizov. On the form of a ship of minimum total resistance (in Russian). unpublished, 1960.
[22] N. Kuznetsov, V. Maz'ya, and B. Vainberg. *Linear water waves*. Cambridge University Press, Cambridge, 2002.
[23] A. Laurain. Distributed and boundary expressions of first and second order shape derivatives in nonsmooth domains. *J. Math. Pures Appl. (9)*, 134:328–368, 2020.
[24] Z. Lian-en. Optimal ship forms for minimal total resistance in shallow water. *Schriftenreihe Schiffbau*, 445:1–60, 1984.
[25] J. H. Michell. The wave resistance of a ship. *Phil. Mag.*, 5(45):106–123, 1898.
[26] F. C. Michelsen. *Wave resistance solution of Michell's integral for polynomial ship forms*. PhD thesis, The University of Michigan, 1960.
[27] J. Nocedal and S. Wright. *Numerical optimization*. Springer Series in Operations Research. Springer-Verlag, New York, 1999.
[28] A. Novruzi and M. Pierre. Structure of shape derivatives. *J. Evol. Equ.*, 2(3):365–382, 2002.
[29] A. Novruzi and J. R. Roche. Newton's method in shape optimisation: a three-dimensional case. *BIT*, 40(1):102–120, 2000.
[30] O. Pironneau. *Optimal shape design for elliptic systems*. Springer Series in Computational Physics. Springer-Verlag, New York, 1984.
[31] V. G. Sizov. The seminar on ship hydrodynamics, organized by Professor M. G. Krein. In *Differential operators and related topics, Vol. I (Odessa, 1997)*, volume 117 of *Oper. Theory Adv. Appl.*, pages 9–20. Birkhäuser, Basel, 2000.
[32] L. N. Sretensky. Sur la détermination de la résistance ondulatoire d'un navire se déplaçant à la surface de l'eau d'une profondeur finie. *Comptes Rendus (Doklady) de l'Académie des Sciences de l'URSS*, 2(11)(90):265–267, 1936.
[33] M. S. Tarafder, G. M. Khalil, and S. M. I. Mahmud. Computation of wave-making resistance of Wigley hull form using Michell's integral. *The Institution of Engineers, Malaysia*, 68:33—40, 2007.
[34] V. Thomée. *Galerkin finite element methods for parabolic problems*, volume 25 of *Springer Series in Computational Mathematics*. Springer-Verlag, Berlin, second edition, 2006.
[35] E. O. Tuck, L. Lazauskas, and D. C. Scullen. Sea wave pattern evaluation - Part 1 report: Primary code and test results (surface vessels). Technical report, Applied Mathematics Department, The University of Adelaide, Australia, 1999.
[36] B. Velichkov. *Existence and regularity results for some shape optimization problems*. PhD thesis, Grenoble, 2013.
[37] J.-L. Vie. *Second-order derivatives for shape optimization with a level-set method*. PhD thesis, Paris Est, 2016.
[38] S.-E. Zerrouq. *Optimisation de forme robuste pour la mécanique des solides et des fluides*. PhD thesis, Université de Pau et des Pays de l'Adour, 2022.